Postprint of Journal of Functional Foods, Volume 29, February 2017, Pages 238–247
DOI http://dx.doi.org/10.1016/j.jff.2016.12.033

Effect of metabolites of hydroxytyrosol on protection against oxidative stress and inflammation in human endothelial cells

Sergio Lopez[a,*], Sergio Montserrat-de la Paz[a], Ricardo Lucas[b,c], Beatriz Bermudez[a,d], Rocio Abia[a], Juan C. Morales[b,c], Francisco J.G. Muriana[a,*]

[a]Laboratory of Cellular and Molecular Nutrition, Instituto de la Grasa (CSIC). 41013 Seville, Spain.

[b]Department of Bioorganic Chemistry, Instituto de Investigaciones Químicas (CSIC-Universidad de Sevilla). 41092, Seville, Spain.

[c]Department of Biochemistry and Molecular Pharmacology, Instituto de Parasitología y Biomedicina (CSIC). 18016, Armilla, Granada, Spain.

[d]Department of Cell Biology, School of Biology (University of Seville). 41012, Seville, Spain.

Corresponding authors: Laboratory of Cellular and Molecular Nutrition, Instituto de la Grasa (CSIC), 41013 Seville, Spain. Tel.: +34 954611550; fax: +34 954616790.

E-mail addresses: serglom@ig.csic.es (S. Lopez), delapaz@us.es (S. Montserrat-de la Paz), ricardo.lucas@ipb.csic.es (R. Lucas), bbermudez@us.es (B. Bermudez), abia@ig.csic.es (R. Abia), jcmorales@ipb.csic.es (J.C. Morales), and muriana@ig.csic.es (F.J.G. Muriana).

Abbreviations: AUC, area-under-the-curve; **CCL2**, chemokine (C-C) motif ligand 2; **DAPI**, diamino-fenilindol; **GAPDH**, glyceraldehyde-3-phosphate dehydrogenase;

GCLC, glutamate-cysteine ligase catalytic subunit; **GPx1**, glutathione peroxidase 1; **GSH**, glutathione; **hECs**, human endothelial cells; **HO-1**, heme oxygenase-1; **HPRT**, hypoxantine-guanine phosphoribosyltransferase; **HTyr**, hydroxytyrosol; **HTyr-GLU**, hydroxytyrosol glucuronate metabolites; **HTyr-*O*-GLU**, hydroxytyrosol orto-glucuronate metabolites; **HTyr-SUL**, hydroxytyrosol sulfate metabolites; **ICAM-1**, intercellular adhesion molecule 1; **MPO**, myeloperoxidase; **MTT**, methylthiazolyldiphenyl-tretrazolium bromide; **NF-κB**, nuclear factor kappa B; **PTGS2**, prostaglandin-endoperoxidase synthase 2; **ROS**, reactive oxygen species; **TBDMS**, tert-butyldimethylsilyl; **TNF-α**, tumour necrosis factor alpha; **TPA**, 12-*O*-tetradecanoylphorbol-13-acetate; **VCAM-1**, vascular adhesion molecule 1.

Abstract

The effects of chemically synthesized metabolites (sulfate and glucuronate forms) from hydroxytyrosol (HTyr) on oxidative stress and inflammation were investigated in TNF-α-activated human endothelial cells. HTyr sulfate metabolites decreased reactive oxygen species and prevented the decrease in glutathione, glutathione peroxidase 1, and glutamate-cysteine ligase catalytic subunit and up-regulated heme oxygenase-1 levels. HTyr and all tested HTyr metabolites (HTyr sulfate > HTyr glucuronate > HTyr) suppressed the phosphorylation of nuclear factor kappa B proteins, the gene expression of intercellular and vascular adhesion molecules, E-selectin, chemokine (C-C) motif ligand 2, and prostaglandin-endoperoxidase synthase 2 and the adhesion of human monocytes. In addition, HTyr sulfate metabolites suppressed plantar and ear swelling and myeloperoxidase activity in inflamed ear tissue in mice treated with carrageenan or 12-*O*-tetradecanoylphorbol-13-acetate. This study demonstrates the antioxidant and/or anti-inflammatory properties of HTyr metabolites in TNF-α-activated hECs and in the prevention of acute and chronic inflammation in mice.

Keywords: hydroxytyrosol, metabolites, inflammation, endothelial cells, human, mice.

1. Introduction

Hydroxytyrosol (HTyr) (**Fig. 1**) is the main phenolic compound found in olives and virgin olive oils (Lopez et al., 2014). This naturally occurring compound has been shown to display high antioxidant and anti-inflammatory capacities, which are directly related to a lower occurrence of cardiovascular disease (Sang, Hou, Lambert, & Yang, 2005; Scalbert, Manach, Morand, Remesy, & Jimenez, 2005). The ingestion of virgin olive oil increases HTyr in plasma in a dose-dependent manner after absorption before being excreted in urine (Covas et al., 2006; Covas, de la Torre, & Fito, 2015); however, it increases plasma antioxidant capacity (Bogani, Galli, Villa, & Visioli, 2007) and protects LDL from oxidative stress (Covas et al., 2006).

Approximately 98% of total HTyr travels through the blood vessels in conjugated forms, either from being ingested or intravenously injected, which suggests that HTyr undergoes an extremely extensive first-pass intestinal/hepatic metabolism (de la Torre-Carbot et al., 2007; de la Torre, 2008; Kotronoulas et al., 2013). Therefore, it is likely that the effects attributed to HTyr are indeed related to its metabolized forms (Rodriguez-Morato et al., 2016). HTyr undergoes three main modifications depending on the phase II enzymes involved: methylation, glucuronation, and sulfation (Kotronoulas et al., 2013). In humans, the main metabolites from HTyr found in plasma are 4'-*O*-D-β-glucuronate, 3'-*O*-D-β-glucuronate, and 4'-*O*-sulfate (de la Torre-Carbot et al., 2007). Recent studies have reported that HTyr may be delivered to the lymph as HTyr accompanied by HTyr metabolites in a 2:1 ratio (Catalan et al., 2015). HTyr metabolites have also been shown to protect human enterocyte-like cells against the pro-oxidant effects of oxidized cholesterol (Atzeri et al., 2016).

The endothelium is involved in the early events of arterial stiffness and atherosclerosis (Libby, 2002; Tiong & Brieger, 2005). The endothelium is a dynamic organ that lines the entire vascular system and may act as a "landing strip" for circulating leukocytes when pro-oxidative and pro-inflammatory pathways become activated by internal or external stimuli such as tumour necrosis factor alpha (TNF-α) or LPS, respectively (Libby, 2002; Sarmiento et al., 2014; Tiong & Brieger, 2005). The production of reactive oxygen species (ROS), the down-regulation of antioxidant response genes, and the secretion of pro-inflammatory mediators operate as an inflammatory beacon for leukocytes, whereas the expression of low-strength and high-strength adhesion molecules is involved in the rolling and firm adhesion of leukocytes to the vascular bed of endothelial cells in processes mediated by NF-κB signalling pathways (Lee et al., 2009; Yang et al., 2013).

Today, the biological properties of single HTyr metabolites compared with HTyr on human endothelial cells (hECs) are unknown. This study aimed to synthesize HTyr glucuronate and HTyr sulfate metabolites using a chemical methodology and to evaluate their antioxidant and anti-inflammatory properties relative to those of HTyr in TNF-α-treated hECs. The anti-inflammatory activity in carrageenan and 12-*O*-tetradecanoylphorbol-13-acetate (TPA) models of mouse plantar and ear inflammation was also assessed.

2. Materials and methods

2.1. Synthesis of HTyr metabolites

HTyr and HTyr acetate were obtained from Seprox Biotech (Madrid, Spain). All other chemicals obtained from commercial sources were used without further purification, unless otherwise noted. All reactions were monitored by TLC on plates pre-coated

with silica gel 60 F254 and detected by heating with Mostain [500 mL of 10% H_2SO_4, 25 g of $(NH_4)_6Mo_7O_{24}\cdot 4H_2O$, 1 g $Ce(SO_4)_2\cdot 4H_2O$]. Products were purified by flash chromatography with Merck silica gel 60 (200-400 mesh). Metabolites were purified by chromatography with C18-reversed phase (RP) silica gel. High-resolution mass spectra were obtained on an ESI/quadrupole AutoSpec-Q mass spectrometer. NMR spectra were recorded on a 300 or 500 MHz spectrometer at room temperature for solutions in $CDCl_3$, D_2O or CD_3OD. 2D NMR experiments (COSY, TOCSY, ROESY, and HMQC) were carried out when necessary to assign the corresponding signals of the new compounds. Sephadex G-25 ion-exchanged with Dowex 50W was used in the purification of glucuronate metabolites. Samples were lyophilized to dryness three times from D_2O to deuterate all exchangeable protons. Raw data were multiplied by a shifted exponential window function prior to Fourier transformation, and the baseline was corrected using polynomial fitting. For details on the synthesis of HTyr glucuronate and sulfate metabolites, see the supplementary material (Supplementary Materials and Methods).

2.2. Cell cultures

hECs (human umbilical vein endothelial cells) were obtained from Lonza (CC2517A; Basel, Switzerland) and grown in EBM-2 medium (Lonza, CC-3156) supplemented with the SingleQuot Kit (Lonza, CC-4176) up to the fifth passage. The human monocytic cell line THP-1 was obtained from the American Type Culture Collection (TIB-202; Rockville, MD, USA) and grown in RPMI-1640 medium containing 10% FBS, 2 mM glutamine, 100 U/mL penicillin, and 0.1 mg/mL streptomycin. Cells were checked for possible mycoplasma contamination using the fluorescent dye diamino-fenilindol (DAPI) (Sigma-Aldrich) and examined under a motorized inverted

fluorescent microscope IX81 equipped with a 100× objective and a Megaview-II digital camera (Olympus, Tokyo, Japan).

2.3. Cell viability assay

hECs were cultured in 96-well plates in eight replicate sets at a density of 10^4 cells per well in the presence of HTyr and HTyr metabolites at the indicated concentrations for 48 h. Cell viability was assayed based on the ability of live cells to reduce methylthiazolyldiphenyl-tretrazolium bromide (MTT) (Jaramillo et al., 2010).

2.4. ROS analysis

The intracellular ROS was determined using the CellROX Green Reagent (ThermoFisher Scientific, Madrid, Spain). hECs were exposed to HTyr or its metabolites (100 μM) for 16 h. Thereafter, cells were treated with TNF-α (10 ng/mL; Preprotech, Rocky Hill, NJ, USA) for 1 h and then with CellROX Green Reagent (5 μM) for 30 min. Cells were washed with PBS and fixed with 3.7% formaldehyde, and the fluorescence signal was analysed in a Fluoroskan Microplate Fluorometer (ThermoFisher Scientific) equipped with a 485/555 excitation/emission filter set. The auto-fluorescence of cells was measured under the same conditions but without adding CellROX Green Reagent.

2.5. GSH assay

hECs were exposed to HTyr or its metabolites (100 μM) for 16 h. Thereafter, cells were treated with TNF-α (10 ng/mL) for 24 h. Cell extracts were obtained in 5% sulfosalicylic acid followed by two freeze/thaw cycles (Yan, Liang, Li, & Zheng, 2015). GSH was determined in samples of cell extracts by measuring the formation of *p*-

nitrophenol from 5,5'-dithiobis (2-nitrobenzoic acid) in the presence of GSH reductase and the reduced form of nicotinamide adenine dinucleotide phosphate according to the GSH Assay Kit (CS0260; Sigma-Aldrich).

2.6. RNA isolation and real-time quantitative PCR analysis

hECs were exposed to HTyr or its metabolites (100 μM) for 16 h. Thereafter, cells were treated with TNF-α (10 ng/mL) for 3 h. The mRNA levels for specific genes were determined by real-time quantitative PCR using a MX3000P system (Stratagene, La Jolla, CA, USA). Total RNA was extracted from cells with TRIsureTM Reagent (Bioline GmbH, Berlin, Germany). RNA quality was assessed using the OD_{260} to OD_{280} ratio, as measured by a NanoDrop ND-1000 Spectrophotometer (ThermoFisher Scientific). Reverse transcription was performed using 1 μg of RNA and iScript Reverse Transcription Kit (Bio-Rad Laboratories, Madrid, Spain). The cDNA template was added to Brilliant SYBR green QPCR Master Mix (Agilent Technologies, Santa Clara, CA, USA) containing the primer pairs for glutathione peroxidase 1 (GPX1), glutamate-cysteine ligase catalytic subunit (GCLC), heme oxygenase-1 (HO-1), intercellular adhesion molecule-1 (ICAM-1), vascular adhesion molecule-1 (VCAM-1), E-selectin, chemokine (C-C) motif ligand 2 (CCL2), prostaglandin-endoperoxidase synthase 2 (PTGS2) or reference genes glyceraldehyde-3-phosphate dehydrogenase (GAPDH) and hypoxantine-guanine phosphoribosyltransferase (HPRT). The sequence and information for the primers used in this study are in presented in the supplementary material (Table S1). Reactions were performed in triplicate, and the change in mRNA expression was calculated using the $2^{-(\Delta\Delta Ct)}$ method. All data were normalized to the endogenous

reference (GAPDH and HPRT) gene levels and expressed as the fold change with respect to the effects of TNF-α.

2.7. Immunoblotting

hECs were exposed to HTyr or its metabolites (100 μM) for 16 h. Thereafter, cells were treated with TNF-α (10 ng/mL) for 3 h for immunoblotting of NF-κB pathway protein members or 6 h for HO-1 and adhesion proteins. Total cell proteins, extracted from hECs under different experimental conditions, were examined by western blot analysis as previously described (Varela et al., 2015). Samples were subjected to SDS-PAGE and transferred onto a nitrocellulose membrane (0.22 μm, Bio-Rad Laboratoires). Protein loading was confirmed by reversible Ponceau S staining. Membranes were immunoblotted with goat anti-HO-1 (C-18, sc-1796; Santa Cruz Biotechnology, Santa Cruz, CA, USA), mouse anti-ICAM-1 (15.2, sc-107), mouse anti-VCAM-1 (E-10, sc-13160), and rabbit anti-E-selectin (H-300, sc-14011) antibodies. The main proteins involved in the NF-κB pathway were also analysed using the NF-κB Pathway Sampler Kit (9936S; Cell Signaling Technology, MA, USA). Specific antigen-antibody complexes were detected with the SuperSignal West Pico Chemiluminescent Substrate (ThermoFisher Scientific, Madrid, Spain). Protein loading equivalence was corrected in relation to the expression of β-tubulin (T4026; Sigma-Aldrich).

2.8. Secretion analysis

hECs were exposed to HTyr or its metabolites (100 μM) for 16 h. Thereafter, cells were treated with TNF-α (10 ng/mL) for 16 h. ICAM-1, VCAM-1, and E-selectin concentrations in culture supernatants were determined by using commercial ELISA

kits (Diaclone, Besancon, France). The values were expressed as pg/mL and calculated from standard curves for each test. DO was measured at 450 nm on a Multiskan Spectrum plate reader (ThermoFisher Scientific).

2.9. Adhesion assay

THP-1 monocytes were labelled with 5 μM calcein-AM (C3100MP; Molecular Probes, Oregon, USA) for 30 min and then seeded (2.5×10^5 cells) over hECs previously exposed to HTyr or its metabolites (100 μM) for 16 h and to TNF-α (10 ng/mL) for additional 6 h. After the co-culture, cells were washed with PBS, and fluorescence was measured at excitation and emission wavelengths of 485 nm and 530 nm, respectively, using a Fluoroskan Microplate Fluorometer (ThermoFisher Scientific). THP-1 cells adhered to hECs were visualized by fluorescence microscopy with a motorized inverted fluorescent microscope IX81 equipped with an FITC filter (Olympus).

2.10. Animals

Forty-eight male Swiss albino mice (*Mus musculus*) aged 5 weeks with a body weight of 20-25 g were used for the present study. The animals were maintained under controlled temperature and light conditions in an animal house and were provided standard mice feed and water *ad libitum*. Mice were divided into 8 groups, with each group containing 5 mice. The dose of HTyr was chosen based on previous studies (Silva et al., 2015). All animal care and experimental procedures complied with the Guidelines of the European Union regarding animal experimentation (Directive of the European Counsel 86/609/EC) and followed a protocol observed and approved by the Animal Ethics Committee of the University of Seville (P09-CVI-5007).

2.11. Carrageenan-induced hind paw oedema

HTyr (0.5 mg/kg) or HTyr-SUL (0.1 and 0.5 mg/kg) was intraperitoneally injected into animals 30 min before the induction of oedema with carrageenan. Oedema was induced by injection of 0.1 mL of a freshly prepared 1% (w/v) carrageenan in sterile saline solution (0.9% NaCl) into the right hind foot of each mouse under the subplantar aponeurosis (Quilez, Montserrat-de la Paz, De la Puerta, Fernández-Arche & García-Giménez, 2015). The control group received sterile saline solution with no carrageenan. The paw volume was measured in mL using a plethysmometer (LE7500; Letica, Madrid, Spain) before carrageenan injection (V_0) and 1, 2, 3, and 5 h post-carrageenan injection (V_t). The increase in volume was taken as the volume of oedema and was calculated as $V_t - V_0$. The area-under-the-curve (AUC) for each experimental condition from 0 to 5 h was calculated by the trapezoidal method.

2.12. TPA-induced ear oedema

Mice were anesthetized with an intraperitoneal injection of sodium pentothal (31.5 mg/kg; Braun, Madrid, Spain). Oedema was then induced by topical application of 20 μL (2.5 μg TPA/ear) dissolved in acetone to both surfaces of the right ear of each mouse (Del-Angel, Nieto, Ramirez-Apan, & Delgado, 2015). Left ears received the same volume of acetone and were maintained as respective controls. HTyr (0.5 mg/kg) or HTyr-SUL (0.1 and 0.5 mg/kg) was topically applied to animals immediately after TPA application. Inflammation was allowed to develop for 24 h, after which the animals were euthanized by cervical dislocation, and disk sections (6 mm diameter) of the central portion of both ears were obtained and weighed. The

oedema, which represented inflammation, was defined as the difference in weight between the disks from right (treated) and left (negative control) ears.

2.13. MPO activity assay

Ear tissue samples (disks) were homogenized in PBS (pH 6.0) containing 0.5% hexadecyltrimethylammonium bromide and were centrifuged at 13000 *g* for 30 min at 4 °C (Del-Angel et al., 2015). MPO activity was measured in collected supernatants according to the method of Bradley et al. (Bradley, Christensen, & Rothstein, 1982). Enzyme activity was determined by measuring OD at 450 nm. Activity is expressed as OD/biopsy.

2.14. Statistical analysis

The data are presented as the mean ± SD. The homogeneity of variance was tested with Bartlett's test. For *in vitro* data, group statistical comparisons were performed by a 1-way ANOVA with a Tukey *post-hoc* test. For *in vivo* data, group statistical comparisons were performed by a Kruskal-Wallis test with a Dunns *post-hoc* test or a 2-way ANOVA with a Bonferroni *post-hoc* test when appropriate. A value of $p < 0.05$ was considered statistically significant.

3. Results

3.1. Synthesis of HTyr metabolites

Glycosylation of HTyr derivative acceptor **7** and glucuronosyl donor **8** was performed using $BF_3{\cdot}OEt_2$ as the promoter (Scheme 1). The corresponding protected HTyr derivatives **9** and **10** were obtained as a regioisomeric mixture in a 51% yield. After deprotection of all the acetyl groups under basic hydrolysis (Na_2CO_3, MeOH, H_2O), a

1.7:1 regioisomeric mixture of HTyr 4'-*O*-β-D-glucuronide (**2**) and HTyr 3'-*O*-β-D-glucuronide (**3**) could be isolated in high yield (88%). Hereinafter, these metabolites **2** and **3** are referred to as HTyr-GLU, with the retained hydroxyl group of the 2-hydroxyethyl side-chain at position 4. A tri-*O*-benzoyl glucuronide derivative of HTyr (**12**) was prepared by glycosylation of the ketal-protected HTyr **11** with the glucuronosyl donor **8** in dry CH_2Cl_2 and $BF_3{\cdot}OEt_2$ as the promoter (Scheme 2). Deprotection of compound **12** was performed in two steps by treatment with Na_2CO_3 to remove the benzoyl groups and then TFA in a mixture of H_2O-THF to remove the acetal group, resulting in HTyr 1-*O*-β-D-glucuronide (**4**) (87% yield). Hereinafter, this metabolite **4** is referred to as HTyr-*O*-GLU, with the retained catecholic hydroxyl groups. Both HTyr-GLU and HTyr-*O*-GLU are referred to as HTyr glucuronate metabolites.

HTyr sulfate metabolites **5** and **6** have been synthesized using protection-deprotection strategies together with the use of microwaves in the critical sulfation step. Hydroxyls of HTyr acetate (**7**) were mono-silyl protected with tert-butyldimethylsilyl (TBDMS) (Scheme 3). The chromatographic separation afforded a 1:1 regioisomeric mixture of the two possible mono-phenolic compounds **13** and **14**. Microwave-assisted sulfation was carried out by treatment with the $SO_3{\cdot}NMe_3$ complex and triethylamine in acetonitrile at 100 °C to obtain a 1:1 mixture of isomers **15** and **16**. Acetyl and silyl deprotection in one step using KF and K_2CO_3 in MeOH resulted in a mixture of HTyr sulfate metabolites **5** and **6** (90% yield). Hereinafter, these metabolites **5** and **6** are referred to as HTyr-SUL, with the retained hydroxyl group of the 2-hydroxyethyl side-chain at position 4, or HTyr sulfate metabolites.

3.2. HTyr and HTyr metabolites on viability of hECs

The viability of hECs was tested at different concentrations (0-200 μM) of HTyr, HTyr-GLU, HTyr-*O*-GLU, and HTyr-SUL for 48 h (Supplementary material [Figure S1]). More than 95% of hECs were able to survive at HTyr or HTyr metabolite concentrations up to 100 μM. A similar concentration has been used in previous studies *in vitro* (Carluccio et al., 2003; Scoditti et al., 2012; Tome-Carneiro et al., 2013) to explore the biological effects of HTyr and other polyphenols, and it was selected for further assays.

3.3. HTyr and HTyr sulfate metabolites suppress TNF-α-induced intracellular production of ROS, depletion of GSH, and down-regulation of genes encoding antioxidant enzymes in hECs

HTyr and HTyr-SUL metabolites but not any of the HTyr glucuronate metabolites suppressed the intracellular production of ROS induced by TNF-α in hECs ($p < 0.05$, Fig. 2A). In line with these effects, HTyr and HTyr-SUL metabolites prevented the depleted intracellular GSH levels ($p < 0.05$, Fig. 2B) and the down-regulated ($p < 0.05$) mRNA levels of GPX1 (Fig. 2C) and GCLC (Fig. 2D) genes. It was observed that HTyr and to a lesser extent HTyr-SUL metabolites markedly induced ($p < 0.05$) the protein and gene expression of HO-1 (Figs. 2E and 2F).

3.4. HTyr and its metabolites suppress TNF-α-induced phosphorylation of NF-κB signalling proteins in hECs

The effects of HTyr and its metabolites on TNF-α-induced NF-κB signalling in hECs was determined by western blot analysis ($p < 0.05$, Fig. 3A). HTyr glucuronate metabolites and most notably HTyr and HTyr sulfate metabolites prevented ($p < 0.05$) the phosphorylation of IKKαβ (Figs. 3B and 3C), IκBα (Fig. 3D), and p65 (Fig. 3E).

3.5. HTyr and its metabolites suppress TNF-α-induced up-regulation of adhesion molecules, CCL2, and PTGS2 genes in hECs

HTyr and its metabolites suppressed ($p < 0.05$) the up-regulation of ICAM-1 (Fig. 4A), VCAM-1 (Fig. 4B), and E-selectin (Fig. 4C) genes induced by TNF-α in hECs. Similar effects were found at the protein level (**Fig. 4D**). Notably, HTyr glucuronate and sulfate metabolites, without differences among them, had more powerful effects than HTyr and even reduced the levels of adhesion molecule genes below those observed in control cells. Accordingly, HTyr and its metabolites suppressed the release of soluble ICAM-1, VCAM-1, and E-selectin (Supplementary material [Table S2]). The increase in the transcriptional activity of genes encoding the monocyte chemoattractant protein-1 (Fig. 4E) and the pro-inflammatory cyclooxygenase-2 (Fig. 4F) were also prevented ($p < 0.05$) by HTyr glucuronate and sulfate metabolites. HTyr had a similar effect on the PTGS2 gene but was ineffective in regulating the CCL2 gene.

3.6. HTyr and its metabolites reduce TNF-α-induced adhesion of monocytes to hECs

HTyr glucuronate metabolites and most notably HTyr and HTyr-SUL metabolites reduced ($p < 0.05$) the adhesion of human THP-1 monocytes induced by TNF-α in hECs (Supplementary material, Figs. S2A and S2B). The adhesion levels with HTyr and HTyr-SUL metabolites did not reach those observed in control cells.

3.7. HTyr and most notably HTyr sulfate metabolites reduce carrageenan-induced paw oedema and TPA-induced ear oedema in mice

The anti-inflammatory effects of HTyr and HTyr-SUL metabolites, as the most active metabolites against TNF-α-induced oxidative and inflammatory response *in vitro*, were also explored in a mouse model of acute (carrageenan) and chronic (TPA) inflammation. Fig. 5A shows that sub-plantar injection of carrageenan produced a prominent increase ($p < 0.05$) in paw thickness, reaching a peak after 2 h. This effect was reduced ($p < 0.05$) after intraperitoneal injection of HTyr and HTyr-SUL metabolites. The AUC value for paw oedema after HTyr-SUL metabolites at a dose of 0.1 mg/kg was similar to that after HTyr at a dose of 0.5 mg/kg (Fig. 5B). As shown in Fig. 5C, the increased ear disk weight induced by TPA was diminished ($p < 0.05$) after topical application of HTyr and HTyr-SUL metabolites, as observed in the mouse carrageenan model. Interestingly, biopsies from ears treated with HTyr and HTyr-SUL metabolites had reduced MPO activity ($p < 0.05$, Fig. 5D). This effect was dose-dependent with HTyr-SUL metabolites ($p < 0.05$).

4. Discussion

In the current study, we synthesized HTyr glucuronate and sulfate metabolites by a chemical methodology and explored their potential antioxidant and anti-inflammatory properties relative to those of HTyr in TNF-α-treated hECs. In previous studies, the ingestion of a commercial preparation of olive mill wastewater or olive extracts rich in HTyr was shown to increase GSH concentration in plasma and skeletal muscle of healthy subjects (Bast & Haenen, 2015; Visioli, Wolfram, Richard, Abdullah, & Crea, 2009). HTyr was also reported to promote the up-regulation of GSH-dependent metabolic processes in adipose tissue of mice fed on a chow diet and the production and release of GSH in the cell supernatant of H_2O_2-treated murine 3T3-L1 adipocytes (Giordano, Davalos, & Visioli, 2014). Other reports have addressed that HTyr

positively regulates the transcriptional activity of HO-1 gene in resting human retinal pigment epithelial cells and porcine vascular endothelial cells (Zou et al., 2012; Zrelli, Kusunoki, & Miyazaki, 2015). In our study, HTyr and HTyr-SUL but not HTyr glucuronate metabolites prevented the TNF-α-induced decrease in GPX1 and GCLC gene expression and GSH production in hECs. GPX1 is an antioxidant enzyme known to catalyse the reduction of H_2O_2 to water and lipid peroxides to their corresponding alcohols (Stefanson & Bakovic, 2014), and GCLC enzyme is the rate-limiting step for the synthesis of the most abundant intracellular antioxidant protein, GSH (Stefanson & Bakovic, 2014; Zhang, 2012). In agreement with these effects, the intracellular ROS levels were not increased in response to TNF-α in HTyr or HTyr-SUL pre-treated hECs. We also recently noticed that HTyr sulfate metabolites are efficient in protecting against the oxidizing action of oxidized cholesterol in human intestinal Caco-2 cells (Atzeri et al., 2016). It was noteworthy that any property of HTyr to scavenge intracellular ROS or to directly modulate the transcriptional activity of GPX1 and GCLC genes and GSH stores was abolished by the conjugation of one of its catecholic hydroxyls or its hydroxyl in the 2-hydroxyethyl side-chain with glucuronic acid. In cell-free systems, the impairment of the antioxidant activity of HTyr (Khymenets et al., 2010) and of the phenolic compounds mangiferin (van der Merwe et al., 2012), resveratrol (Lu et al., 2013), and quercetin (Messer, Hopkins, & Kipp, 2015) due to their glucuronidation supported this finding. However, glucuronide metabolites of HTyr may protect renal cell membranes against lipid peroxidation induced by external injury with H_2O_2 (Deiana et al., 2011) and may inhibit tunicamycin-induced endoplasmic reticulum stress in human hepatic HepG2 cells (Giordano, Dangles, Rakotomanomana, Baracchini, & Visioli, 2015). Our observations likely suggest that the catechol moiety in HTyr represents a structural

requirement to preserve hECs against TNF-α-induced oxidative stress that is not damaged by the conjugation with sulfuric acid because HTyr sulfate metabolites exhibited antioxidant effects comparable to those of the parent HTyr molecule. The dramatic up-regulation of HO-1 mRNA and protein levels induced by HTyr, and to a lesser extent by HTyr-SUL, in TNF-α-treated hECs is also indicative of specific and distinctive mechanisms by which HTyr and its sulfate metabolites powerfully stimulate host defence against oxidative stress. HO-1 enzyme, the rate-limiting step in the catabolism of heme into the bioactive signalling molecules carbon monoxide, biliverdin, and iron, is receiving growing attention as a master cytoprotective sentinel (Otterbein, Foresti, & Motterlini, 2016). Expression of HO-1 has potent anti-apoptotic effects in ECs (Brouard et al., 2000), and the 5′-UTR of the human HO-1 gene contains many stress-activated response elements, including an NF-κB site (Rushworth, Bowles, Raninga, & MacEwan, 2010), and antioxidant response elements that trigger the transcription of more than 200 endogenous protective genes encoding antioxidant, phase II detoxification, and anti-inflammatory co-stimulating proteins, and molecular chaperones (Chen, Lu, Chen, & Cheng, 2015). HTyr and HTyr-SUL metabolite treatments were nontoxic to hECs under our experimental conditions, indicating that the observed up-regulation of HO-1 does not involve nonspecific cytotoxic mechanisms. Therefore, our findings led to the notion that HO-1 targeting by HTyr and HTyr-SUL could be beneficial for decreasing endothelium vulnerability to attack by oxidative stimuli.

TNF-α is predominantly produced by macrophages, and its capability to stimulate intracellular ROS production also involves NF-κB activation and the transcription of pro-inflammatory genes in endothelial cells (Parameswaran & Patial, 2010). NF-κB activity is regulated by IκB proteins (mainly IκBα in endothelial cells)

and IκB kinases (IKKα and IKKβ). These IκB kinases mediate the phosphorylation of IκBα, an important step in NF-κB activation that leads to the release of NF-κB dimers from the cytoplasmic NF-κB-IκB complex and to the phosphorylation and translocation of NF-κB family of transcription factors, mainly of its subunit p65 into the nucleus. Following stimulation with TNF-α, HTyr and its metabolites down-regulated the TNF-α-induced NF-κB signalling in hECs by reducing protein levels of phosphorylated IKKα, IKKβ, IκBα, and p65. HTyr and HTyr-SUL were the most efficient inhibitors of NF-κB activation. However, all of the HTyr metabolites, with no differences among them, were more efficient than HTyr in inhibiting TNF-α-induced gene expression of adhesion molecules ICAM-1, VCAM-1, E-selectin, the chemokine CCL2, and the enzyme COX-2 in hECs. Furthermore, all tested molecules diminished THP-1 monocyte adhesion to hECs, with HTyr and HTyr-SUL exerting more potent effects than HTyr glucuronate metabolites. These findings strengthen the idea that HTyr metabolites produce anti-inflammatory effects in TNF-α-treated hECs and that the potency of these effects depends on the place and type of modification in the HTyr structure. Although our study is the first to quantitatively establish the preventive properties of HTyr-SUL, HTyr-GLU, and HTyr-*O*-GLU metabolites compared with HTyr on human endothelial activation, our results are in agreement with previous reports showing suppressive effects of HTyr on LPS-, TNF-α- and PMA-induced activation of VCAM-1 gene expression and LPS-induced NF-κB activation, ICAM-1 and E-selectin gene expression, and U937 cell adhesion in hECs (Carluccio et al., 2003). HTyr was also reported to suppress PMA-induced COX-2 gene expression in hECs (Scoditti et al., 2012) and TNF-α-induced NF-κB activation in hECs (Dell'Agli et al., 2006) and porcine ECs (Zrelli, Wu, Zghonda, Shimizu, & Miyazaki, 2013).

Inspired by these observations and our previous study supporting the acute vascular anti-inflammatory effects of virgin olive oil in healthy subjects and in subjects with a high fasting triacylglycerol concentration (Pacheco et al., 2007), we measured the effects of HTyr and HTyr-SUL on the course of inflammation in the carrageenan-induced paw oedema in mice and found that HTyr-SUL was more effective than HTyr in reducing paw swelling. We also observed that HTyr-SUL was more potent than HTyr in reducing the size of oedema induced by TPA in mouse ears. In the carrageenan and TPA models, it is known that local inflammation occurs with the generation of ROS, inflammatory mediators such as TNF-α, and leukocyte infiltration (Sadeghi et al., 2014). Noticeably, HTyr-SUL decreased MPO activity (as an index of leukocyte infiltration) in a dose-dependent fashion in the ear of TPA-treated mice. In support of these observations, HTyr supplementation was recently reported to reduce inflammation in rats injected with carrageenan or collagen (Quilez, Montserrat-de la Paz, De la Puerta, Fernández-Arche & García-Giménez, 2015). Therefore, our findings suggest that the abovementioned *in vitro* antioxidant and anti-inflammatory activities of HTyr-SUL could participate, at least partly, in its *in vivo* anti-oedematogenic activity.

The present study has certain strengths and limitations. One strength is that we compared the biological effects of HTyr and its most important metabolites. A limitation is that the concentration of HTyr and HTyr metabolites used for this purpose is higher than the concentrations described in human plasma after a single ingestion of virgin olive oil.

5. Conclusions

In summary, this study reveals biological properties of HTyr metabolites in hECs. We demonstrated that HTyr metabolites ameliorate the TNF-α-induced oxidative (HTyr sulfate metabolites = HTyr) and inflammatory (HTyr sulfate metabolites > HTyr glucuronate metabolites > HTyr) status of hECs. We also provide *in vivo* evidence of HTyr sulfate metabolites ameliorating inflammation. Together, these findings reflect the potential of HTyr metabolites, notably HTyr-SUL, as promising anti-inflammatory therapeutic agents and offer novel mechanistic explanations underlying the benefits derived from the consumption of virgin olive oil in the prevention of atherosclerotic disease and other inflammatory-related conditions.

Conflict of interest

The authors have declared no conflicts of interest.

Acknowledgements

This study was funded by research grant P09-CVI-5007 (Junta de Andalucía, Spain). Contracts for R.L. and Angela Palma Pacheco (technician) were also supported by P09-CVI-5007. S.M. has the benefit of a FPI fellowship (BES-2012-056104) of MICINN. S.L. acknowledges a contract cofunded by the European Social Fund (ESF) from the Spanish MINECO (JCI-2012-13084, Juan de la Cierva) and the Spanish Research Council (CSIC)/JAEdoc Program (JAEDOC089). B.B. acknowledges funds from the “V Own Research Plan” (University of Seville).

References

Atzeri, A., Lucas, R., Incani, A., Penalver, P., Zafra-Gomez, A., Melis, M. P.,Pizzala, R., Morales, J. C., & Deiana, M. (2016). Hydroxytyrosol and tyrosol sulfate

metabolites protect against the oxidized cholesterol pro-oxidant effect in Caco-2 human enterocyte-like cells. *Food and Function, 7*(1), 337-346.

Bast, A., & Haenen, G. (2015). Nutritional Antioxidants: It Is Time to Categorise. In M. Lamprecht (Ed.), *Antioxidants in Sport Nutrition*. Boca Raton (FL): CRC Press/Taylor & Francis(c) 2015 by Taylor & Francis Group, LLC.

Bogani, P., Galli, C., Villa, M., & Visioli, F. (2007). Postprandial anti-inflammatory and antioxidant effects of extra virgin olive oil. *Atherosclerosis, 190*(1), 181-186.

Bradley, P. P., Christensen, R. D., & Rothstein, G. (1982). Cellular and extracellular myeloperoxidase in pyogenic inflammation. *Blood, 60*(3), 618-622.

Brouard, S., Otterbein, L. E., Anrather, J., Tobiasch, E., Bach, F. H., Choi, A. M., & Soares, M. P. (2000). Carbon monoxide generated by heme oxygenase 1 suppresses endothelial cell apoptosis. *Journal of Experimental Medicine, 192*(7), 1015-1026.

Carluccio, M. A., Siculella, L., Ancora, M. A., Massaro, M., Scoditti, E., Storelli, C., Visioli, F., Distante, A., & De Caterina, R. (2003). Olive oil and red wine antioxidant polyphenols inhibit endothelial activation: antiatherogenic properties of Mediterranean diet phytochemicals. *Arteriosclerosis, Thrombosis, and Vascular Biology, 23*(4), 622-629.

Catalan, U., Lopez de Las Hazas, M. C., Rubio, L., Fernandez-Castillejo, S., Pedret, A., de la Torre, R., Motilva, M. J., & Sola, R. (2015). Protective effect of hydroxytyrosol and its predominant plasmatic human metabolites against endothelial dysfunction in human aortic endothelial cells. *Molecular Nutrition and Food Research, 59*(12), 2523-2536.

Chen, B., Lu, Y., Chen, Y., & Cheng, J. (2015). The role of Nrf2 in oxidative stress-induced endothelial injuries. *Journal of Endocrinology, 225*(3), R83-99.

Covas, M. I., de la Torre, K., Farre-Albaladejo, M., Kaikkonen, J., Fito, M., Lopez-Sabater, C., Pujadas-Bastardes, M. A., Joglar, J., Weinbrenner, T., Lamuela-Raventós, R. M., & de la Torre, R. (2006). Postprandial LDL phenolic content and LDL oxidation are modulated by olive oil phenolic compounds in humans. *Free Radical Biology and Medicine, 40*(4), 608-616.

Covas, M. I., de la Torre, R., & Fito, M. (2015). Virgin olive oil: a key food for cardiovascular risk protection. *British Journal of Nutrition, 113*(Suppl 2), S19-28.

de la Torre-Carbot, K., Chavez-Servin, J. L., Jauregui, O., Castellote, A. I., Lamuela-Raventos, R. M., Fito, M., Covas, M. I., Muñoz-Aguayo, D., & Lopez-Sabater, M. C. (2007). Presence of virgin olive oil phenolic metabolites in human low density lipoprotein fraction: determination by high-performance liquid chromatography-electrospray ionization tandem mass spectrometry. *Analytica Chimica Acta, 583*(2), 402-410.

de la Torre, R. (2008). Bioavailability of olive oil phenolic compounds in humans. *Inflammopharmacology, 16*(5), 245-247.

Deiana, M., Incani, A., Rosa, A., Atzeri, A., Loru, D., Cabboi, B., Paola Melis, M., Lucas, R., Morales, J. C., & Assunta Dessi, M. (2011). Hydroxytyrosol glucuronides protect renal tubular epithelial cells against H(2)O(2) induced oxidative damage. *Chemico-Biological Interactions, 193*(3), 232-239.

Del-Angel, M., Nieto, A., Ramirez-Apan, T., & Delgado, G. (2015). Anti-inflammatory effect of natural and semi-synthetic phthalides. *European Journal of Pharmacology, 752*, 40-48.

Dell'Agli, M., Fagnani, R., Mitro, N., Scurati, S., Masciadri, M., Mussoni, L., Galli, G.V., Bosisio, E., Crestani, M., De Fabiani, E., Tremoli, E., & Caruso, D.

(2006). Minor components of olive oil modulate proatherogenic adhesion molecules involved in endothelial activation. *Journal of Agricultural and Food Chemistry, 54*(9), 3259-3264.

Giordano, E., Dangles, O., Rakotomanomana, N., Baracchini, S., & Visioli, F. (2015). 3-O-Hydroxytyrosol glucuronide and 4-O-hydroxytyrosol glucuronide reduce endoplasmic reticulum stress in vitro. *Food and Function, 6*(10), 3275-3281.

Giordano, E., Davalos, A., & Visioli, F. (2014). Chronic hydroxytyrosol feeding modulates glutathione-mediated oxido-reduction pathways in adipose tissue: A nutrigenomic study. *Nutrition Metabolism and Cardiovascular Diseases, 24*(10), 1144-1150.

Jaramillo, S., Lopez, S., Varela, L. M., Rodriguez-Arcos, R., Jimenez, A., Abia, R., Guillen, R., & Muriana, F. J. (2010). The flavonol isorhamnetin exhibits cytotoxic effects on human colon cancer cells. *Journal of Agricultural and Food Chemistry, 58*(20), 10869-10875.

Khymenets, O., Fito, M., Touriño, S., Muñoz-Aguayo, D., Pujadas, M., Torres, J. L., Joglar, J., Farre, M., Covas, M. I., & de la Torre R. (2010). Antioxidant activities of hydroxytyrosol main metabolites do not contribute to beneficial health effects after olive oil ingestion. *Drug Metabolism and Disposition, 38*(9), 1417-1421.

Kotronoulas, A., Pizarro, N., Serra, A., Robledo, P., Joglar, J., Rubió, L., Hernaéz, A., Tormos, C., Motilva, M. J., Fitó, M., Covas, M. I., Solà, R., Farré, M., Saez, G., & de la Torre, R. (2013). Dose-dependent metabolic disposition of hydroxytyrosol and formation of mercapturates in rats. *Pharmacological Research, 77*, 47-56.

Lee, I. T., Luo, S. F., Lee, C. W., Wang, S. W., Lin, C. C., Chang, C. C., Chen, Y. L., Chau, L. Y., & Yang, C. M. (2009). Overexpression of HO-1 protects against TNF-alpha-mediated airway inflammation by down-regulation of TNFR1-dependent oxidative stress. *American Journal of Pathology, 175*(2), 519-532.

Libby, P. (2002). Inflammation in atherosclerosis. *Nature, 420*(6917), 868-874.

Lopez, S., Bermudez, B., Montserrat-de la Paz, S., Jaramillo, S., Varela, L. M., Ortega-Gomez, A., Abia, R., & Muriana, F. J. (2014). Membrane composition and dynamics: a target of bioactive virgin olive oil constituents. *Biochimica et Biophysica Acta, 1838*(6), 1638-1656.

Lu, D. L., Ding, D. J., Yan, W. J., Li, R. R., Dai, F., Wang, Q., Yu, S. S., Jin, X. L., & Zhou, B. (2013). Influence of glucuronidation and reduction modifications of resveratrol on its biological activities. *Chembiochem, 14*(9), 1094-1104.

Messer, J. G., Hopkins, R. G., & Kipp, D. E. (2015). Quercetin Metabolites Up-Regulate the Antioxidant Response in Osteoblasts Isolated From Fetal Rat Calvaria. *Journal of Cellular Biochemistry, 116*(9), 1857-1866.

Otterbein, L. E., Foresti, R., & Motterlini, R. (2016). Heme Oxygenase-1 and Carbon Monoxide in the Heart: The Balancing Act Between Danger Signaling and Pro-Survival. *Circulation Research, 118*(12), 1940-1959.

Pacheco, Y. M., Bemudez, B., Lopez, S., Abia, R., Villar, J., & Muriana, F. J. (2007). Minor compounds of olive oil have postprandial anti-inflammatory effects. *British Journal of Nutrition, 98*(2), 260-263.

Parameswaran, N., & Patial, S. (2010). Tumor necrosis factor-alpha signaling in macrophages. *Critical Reviews in Eukaryotic Gene Expression, 20*(2), 87-103.

Quilez, A. M. Montserrat-de la Paz, S., De la Puerta, R., Fernández-Arche, M.A., & García-Giménez, M.D. (2015). Validation of ethnopharmacological use as anti-

inflammatory of a decoction from Annona Muricata Leaves. *African Journal of Traditional, Complementary and Alternative Medicines, 12*, 14-20.

Rodriguez-Morato, J., Boronat, A., Kotronoulas, A., Pujadas, M., Pastor, A., Olesti, E., Perez-Maña, C., Khymenets, O., Fito, M., Farre, M., & de la Torre, R. (2016). Metabolic disposition and biological significance of simple phenols of dietary origin: hydroxytyrosol and tyrosol. *Drug Metabolism Reviews, 48*(2), 218-236.

Rushworth, S. A., Bowles, K. M., Raninga, P., & MacEwan, D. J. (2010). NF-kappaB-inhibited acute myeloid leukemia cells are rescued from apoptosis by heme oxygenase-1 induction. *Cancer Research, 70*(7), 2973-2983.

Sadeghi, H., Zarezade, V., Akbartabar Toori, M., Jafari Barmak, M., Azizi, A., Ghavamizadeh, M., & Mostafazadeh, M. (2014). Anti-in fl ammatory Activity of Stachys Pilifera Benth. *Iranian Red Crescent Medical Journal, 16*(9), e19259.

Sang, S., Hou, Z., Lambert, J. D., & Yang, C. S. (2005). Redox properties of tea polyphenols and related biological activities. *Antioxidant and Redox Signaling, 7*(11-12), 1704-1714.

Sarmiento, D., Montorfano, I., Caceres, M., Echeverria, C., Fernandez, R., Cabello-Verrugio, C., Cerda, O., Tapia, P., & Simon, F. (2014). Endotoxin-induced vascular endothelial cell migration is dependent on TLR4/NF-kappaB pathway, NAD(P)H oxidase activation, and transient receptor potential melastatin 7 calcium channel activity. *International Journal of Biochemistry and Cell Biology, 55*, 11-23.

Scalbert, A., Manach, C., Morand, C., Remesy, C., & Jimenez, L. (2005). Dietary polyphenols and the prevention of diseases. *Critical Reviews in Food Science and Nutrition, 45*(4), 287-306.

Scoditti, E., Calabriso, N., Massaro, M., Pellegrino, M., Storelli, C., Martines, G., De Caterina, R., & Carluccio, M. A. (2012). Mediterranean diet polyphenols reduce inflammatory angiogenesis through MMP-9 and COX-2 inhibition in human vascular endothelial cells: a potentially protective mechanism in atherosclerotic vascular disease and cancer. *Archives of Biochemistry and Biophysics, 527*(2), 81-89.

Silva, S., Sepodes, B., Rocha, J., Direito, R., Fernandes, A., Brites, D., Freitas, M., Fernandes, E., Bronze, M. R., & Figueira, M. E. (2015). Protective effects of hydroxytyrosol-supplemented refined olive oil in animal models of acute inflammation and rheumatoid arthritis. *Journal of Nutritional Biochemistry, 26*(4), 360-368.

Stefanson, A. L., & Bakovic, M. (2014). Dietary regulation of Keap1/Nrf2/ARE pathway: focus on plant-derived compounds and trace minerals. *Nutrients, 6*(9), 3777-3801.

Tiong, A. Y., & Brieger, D. (2005). Inflammation and coronary artery disease. *American Heart Journal, 150*(1), 11-18.

Tome-Carneiro, J., Larrosa, M., Gonzalez-Sarrias, A., Tomas-Barberan, F. A., Garcia-Conesa, M. T., & Espin, J. C. (2013). Resveratrol and clinical trials: the crossroad from in vitro studies to human evidence. *Current Pharmaceutical Design, 19*(34), 6064-6093.

van der Merwe, J. D., Joubert, E., Manley, M., de Beer, D., Malherbe, C. J., & Gelderblom, W. C. (2012). Mangiferin glucuronidation: important hepatic modulation of antioxidant activity. *Food and Chemical Toxicology, 50*(3-4), 808-815.

Varela, L. M., Lopez, S., Ortega-Gomez, A., Bermudez, B., Buers, I., Robenek, H., . . . Abia, R. (2015). Postprandial triglyceride-rich lipoproteins regulate perilipin-2 and perilipin-3 lipid-droplet-associated proteins in macrophages. *Journal of Nutritional Biochemistry, 26*(4), 327-336.

Visioli, F., Wolfram, R., Richard, D., Abdullah, M. I., & Crea, R. (2009). Olive phenolics increase glutathione levels in healthy volunteers. *Journal of Agricultural and Food Chemistry, 57*(5), 1793-1796.

Yan, X., Liang, F., Li, D., & Zheng, J. (2015). Ouabain elicits human glioblastoma cells apoptosis by generating reactive oxygen species in ERK-p66SHC-dependent pathway. *Molecular and Cellular Biochemistry, 398*(1-2), 95-104.

Yang, Y. C., Lii, C. K., Wei, Y. L., Li, C. C., Lu, C. Y., Liu, K. L., & Chen, H. W. (2013). Docosahexaenoic acid inhibition of inflammation is partially via cross-talk between Nrf2/heme oxygenase 1 and IKK/NF-kappaB pathways. *Journal of Nutritional Biochemistry, 24*(1), 204-212.

Zhang, Y. (2012). Phase II Enzymes. In M. Schwab (Ed.), *Encyclopedia of Cancer* (pp. 2853-2855). Berlin, Heidelberg: Springer Berlin Heidelberg.

Zou, X., Feng, Z., Li, Y., Wang, Y., Wertz, K., Weber, P., Fu, Y., & Liu, J. (2012). Stimulation of GSH synthesis to prevent oxidative stress-induced apoptosis by hydroxytyrosol in human retinal pigment epithelial cells: activation of Nrf2 and JNK-p62/SQSTM1 pathways. *Journal of Nutritional Biochemistry, 23*(8), 994-1006.

Zrelli, H., Kusunoki, M., & Miyazaki, H. (2015). Role of Hydroxytyrosol-dependent Regulation of HO-1 Expression in Promoting Wound Healing of Vascular Endothelial Cells via Nrf2 De Novo Synthesis and Stabilization. *Phytotherapy Research, 29*(7), 1011-1018.

Zrelli, H., Wu, C. W., Zghonda, N., Shimizu, H., & Miyazaki, H. (2013). Combined treatment of hydroxytyrosol with carbon monoxide-releasing molecule-2 prevents TNF alpha-induced vascular endothelial cell dysfunction through NO production with subsequent NFkappaB inactivation. *BioMed Research International, 2013*, 912431.

FIGURE CAPTIONS

Fig. 1. Structure of hydroxytyrosol (HTyr) **1**, HTyr glucuronate metabolites **2-4**, and HTyr sulfate metabolites **5** and **6**.

Fig. 2. Effects of hydroxytyrosol (HTyr), hydroxytyrosol glucuronate metabolites (HTyr-GLU and HTyr-*O*-GLU), and hydroxytyrosol sulfate metabolites (HTyr-SUL) (all 100 μM for 16 h) on the production of intracellular reactive oxygen species (ROS) (A), stores of GSH (B), gene expression of GPX1 (C), GCLC (D), and HO-1 (E), and protein expression of HO-1 (F) in TNF-α-treated hECs. Values are shown as mean ± SD (n = 3). Bars without a common lowercase letter differ ($p < 0.05$).

Fig. 3. Effects of hydroxytyrosol (HTyr), hydroxytyrosol glucuronate metabolites (HTyr-GLU and HTyr-*O*-GLU), and hydroxytyrosol sulfate metabolites (HTyr-SUL) (all 100 μM for 16 h) on the phosphorylation of NF-κB signalling proteins (A), including quantitative analysis of IKKαβ (B, C), IκBα (D), and p65 (E) in TNF-α-treated hECs. Values are shown as mean ± SD (n = 3). Bars without a common lowercase letter differ ($p < 0.05$).

Fig. 4. Effects of hydroxytyrosol (HTyr), hydroxytyrosol glucuronate metabolites (HTyr-GLU and HTyr-*O*-GLU), and hydroxytyrosol sulfate metabolites (HTyr-SUL) (all 100 μM for 16 h) on the gene expression of ICAM-1 (A), VCAM-1 (B), E-selectin (C), protein expression of ICAM-1, VCAM-1, and E-selectin (D), and gene expression of CCL2 (E), and PTGS2 (F) in TNF-α-treated hECs. Values are shown as mean ± SD (n = 3). Bars without a common lowercase letter differ ($p < 0.05$).

Fig. 5. Effects of hydroxytyrosol (HTyr, 0.5 mg/kg) and hydroxytyrosol sulfate metabolites (HTyr-SUL, 0.1 and 0.5 mg/kg) on carrageenan-induced paw oedema volume in mice (A), including areas-under-the curve for paw oedema volume (B), and on TPA-induced ear oedema weight (C) and MPO activity (D) in mice. Values are shown as mean ± SD (n = 5). Relative to paw oedema volume: drug effect, time effect, and interaction effect are all $p<0.05$ (two-way ANOVA). $^{\#}p < 0.05$, carrageenan *vs* all compounds at indicated times (Bonferroni *post-hoc* test). Bars without a common lowercase letter differ ($p < 0.05$).

SCHEME CAPTIONS

Scheme 1. Synthesis of HTyr-GLU metabolites **2** and **3**.

Scheme 2. Synthesis of HTyr-*O*-GLU metabolite **4**.

Scheme 3. Synthesis of HTyr-SUL metabolites **5** and **6**.

Figures 1-5

Fig. 1

Click here to download Figure: Figures JFF 2016 v1.pptx

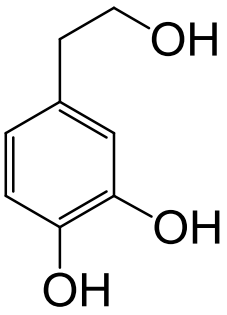

1 (HTyr)

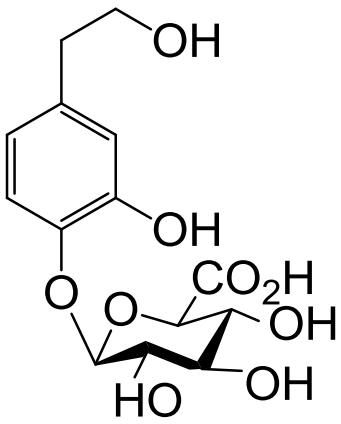

2

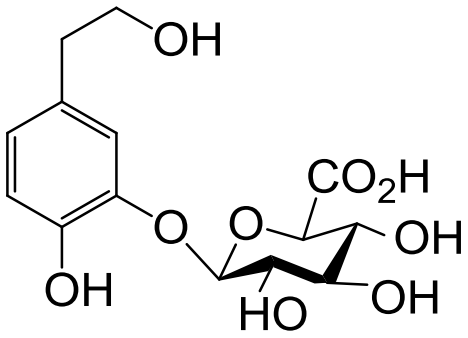

3

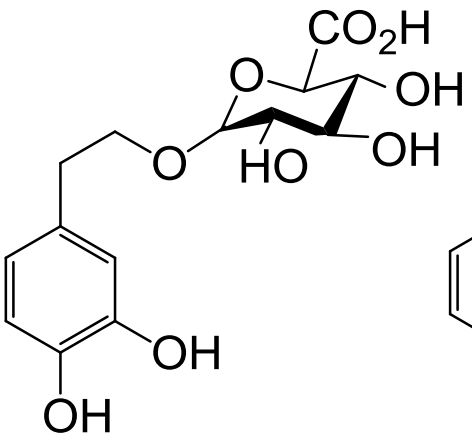

4

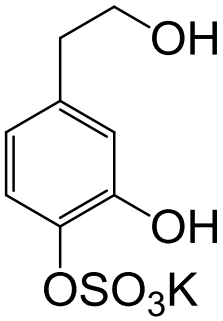

5

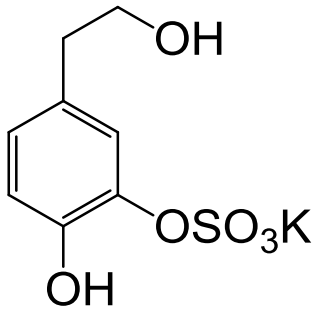

6

Fig. 2

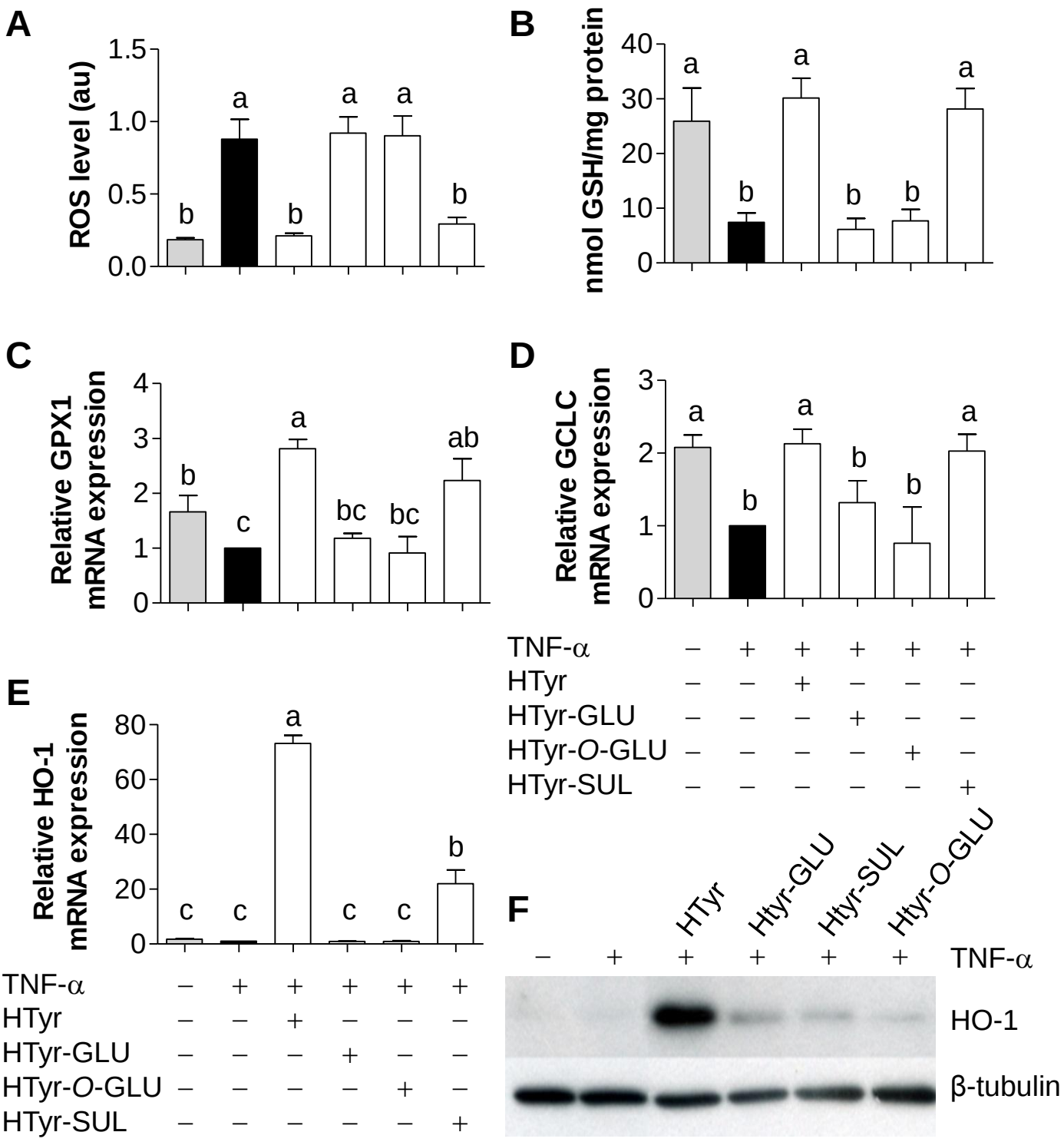
A
ROS level (au)
1.5
1.0
0.5
0.0
b
a
b
a
a
b
B
nmol GSH/mg protein
40
30
20
10
0
a
b
a
b
b
a
C
Relative GPX1 mRNA expression
4
3
2
1
0
b
c
a
bc
bc
ab
D
Relative GCLC mRNA expression
3
2
1
0
a
b
a
b
b
a
TNF-α – + + + + +
HTyr – – + – – –
HTyr-GLU – – – + – –
HTyr-O-GLU – – – – + –
HTyr-SUL – – – – – +
E
Relative HO-1 mRNA expression
80
60
40
20
0
c
c
a
c
c
b
TNF-α – + + + + +
HTyr – – + – – –
HTyr-GLU – – – + – –
HTyr-O-GLU – – – – + –
HTyr-SUL – – – – – +
F
HTyr
Htyr-GLU
Htyr-SUL
Htyr-O-GLU
– + + + + + TNF-α
HO-1
β-tubulin

Fig. 3

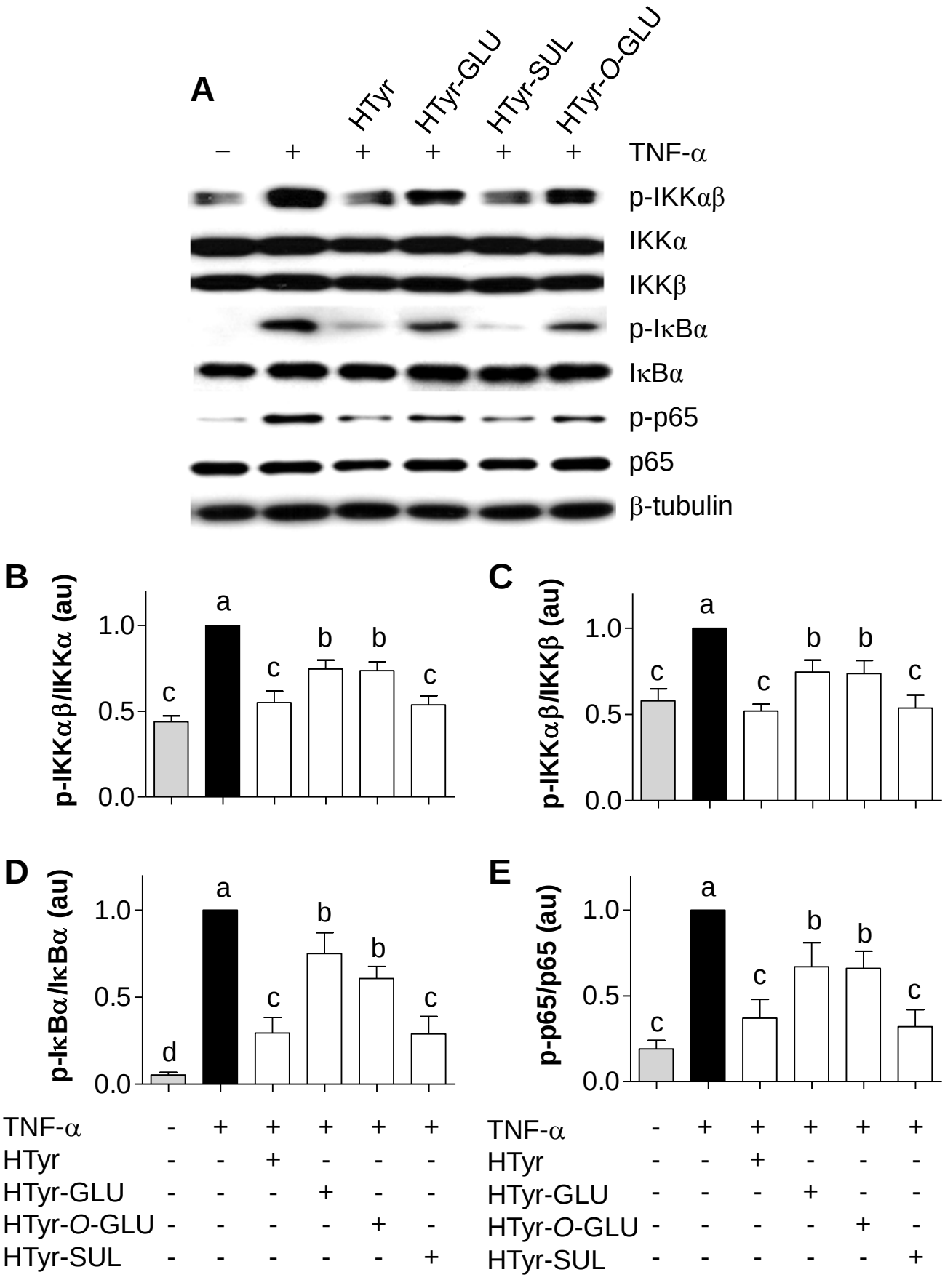
A
HTyr
HTyr-GLU
HTyr-SUL
HTyr-O-GLU
TNF-α
p-IKKαβ
IKKα
IKKβ
p-IκBα
IκBα
p-p65
p65
β-tubulin
B
p-IKKαβ/IKKα (au)
C
p-IKKαβ/IKKβ (au)
D
p-IκBα/IκBα (au)
E
p-p65/p65 (au)
TNF-α
HTyr
HTyr-GLU
HTyr-O-GLU
HTyr-SUL

Fig. 4

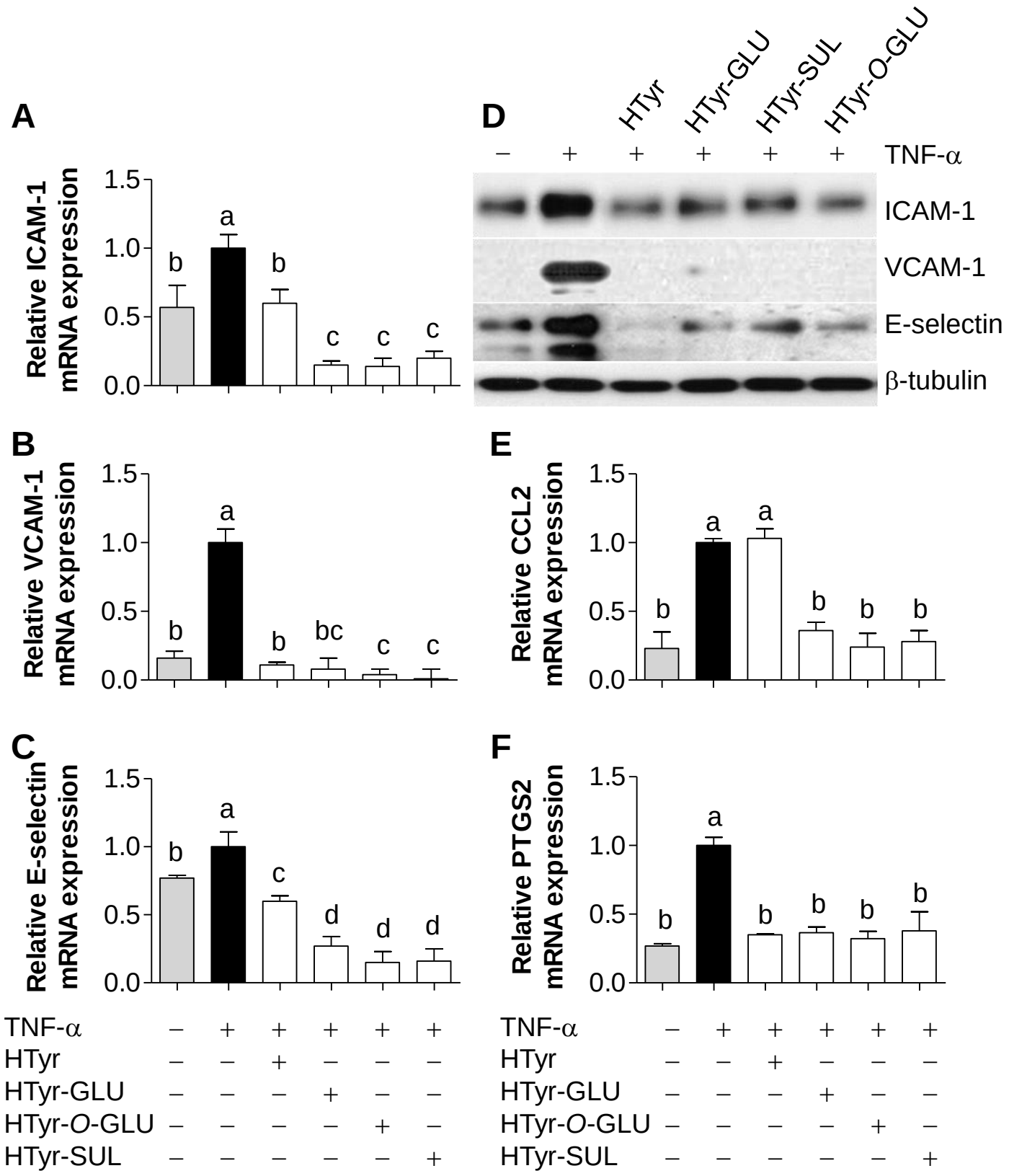
A
Relative ICAM-1 mRNA expression
1.5
1.0
0.5
0.0
a
b
b
c
c
c
D
HTyr
HTyr-GLU
HTyr-SUL
HTyr-O-GLU
TNF-α
ICAM-1
VCAM-1
E-selectin
β-tubulin
B
Relative VCAM-1 mRNA expression
a
b
b
bc
c
c
E
Relative CCL2 mRNA expression
a
a
b
b
b
C
Relative E-selectin mRNA expression
a
b
c
d
d
d
F
Relative PTGS2 mRNA expression
a
b
b
b
b
TNF-α – + + + + +
HTyr – – + – – –
HTyr-GLU – – – + – –
HTyr-O-GLU – – – – + –
HTyr-SUL – – – – – +

Fig. 5

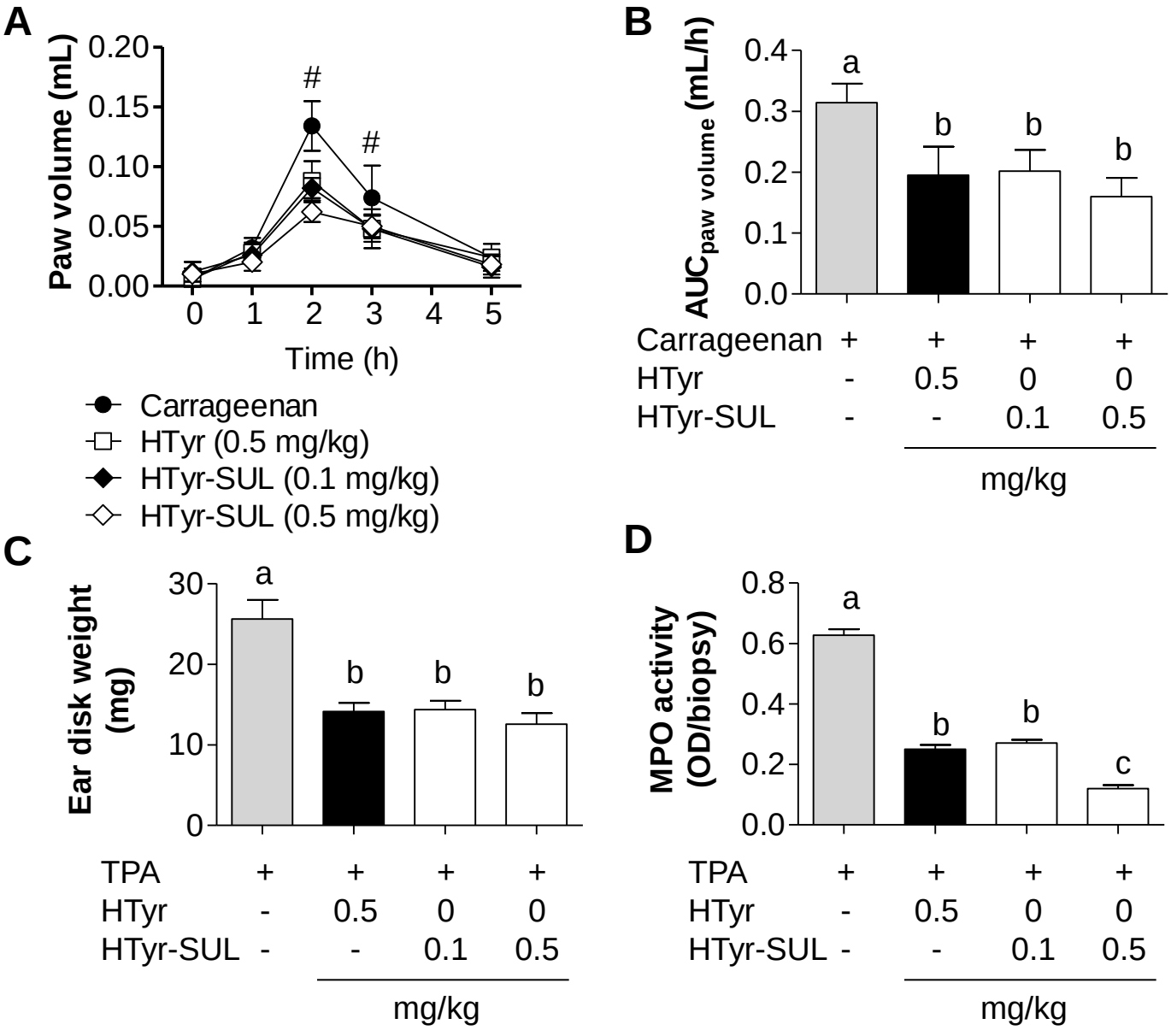
A
Paw volume (mL)
0.20
0.15
0.10
0.05
0.00
0 1 2 3 4 5
Time (h)
#
#
Carrageenan
HTyr (0.5 mg/kg)
HTyr-SUL (0.1 mg/kg)
HTyr-SUL (0.5 mg/kg)
B
AUC paw volume (mL/h)
0.4
0.3
0.2
0.1
0.0
a
b
b
b
Carrageenan + + + +
HTyr - 0.5 0 0
HTyr-SUL - - 0.1 0.5
mg/kg
C
Ear disk weight (mg)
30
20
10
0
a
b
b
b
TPA + + + +
HTyr - 0.5 0 0
HTyr-SUL - - 0.1 0.5
mg/kg
D
MPO activity (OD/biopsy)
0.8
0.6
0.4
0.2
0.0
a
b
b
c
TPA + + + +
HTyr - 0.5 0 0
HTyr-SUL - - 0.1 0.5
mg/kg

Schemes 1-3

Scheme 1

Click here to download Figure: Schemes JFF 2016 v1.pptx

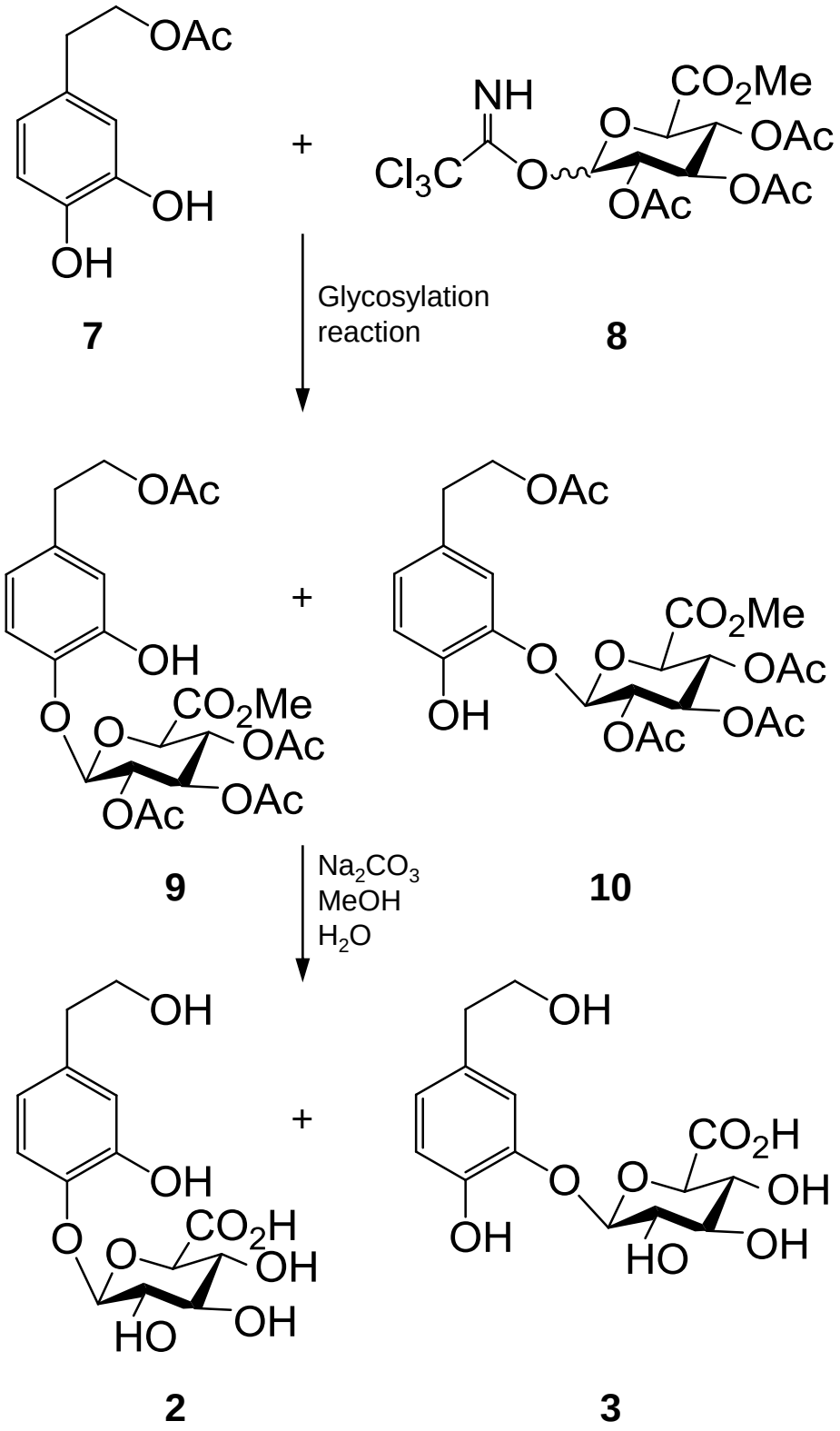

Scheme 2

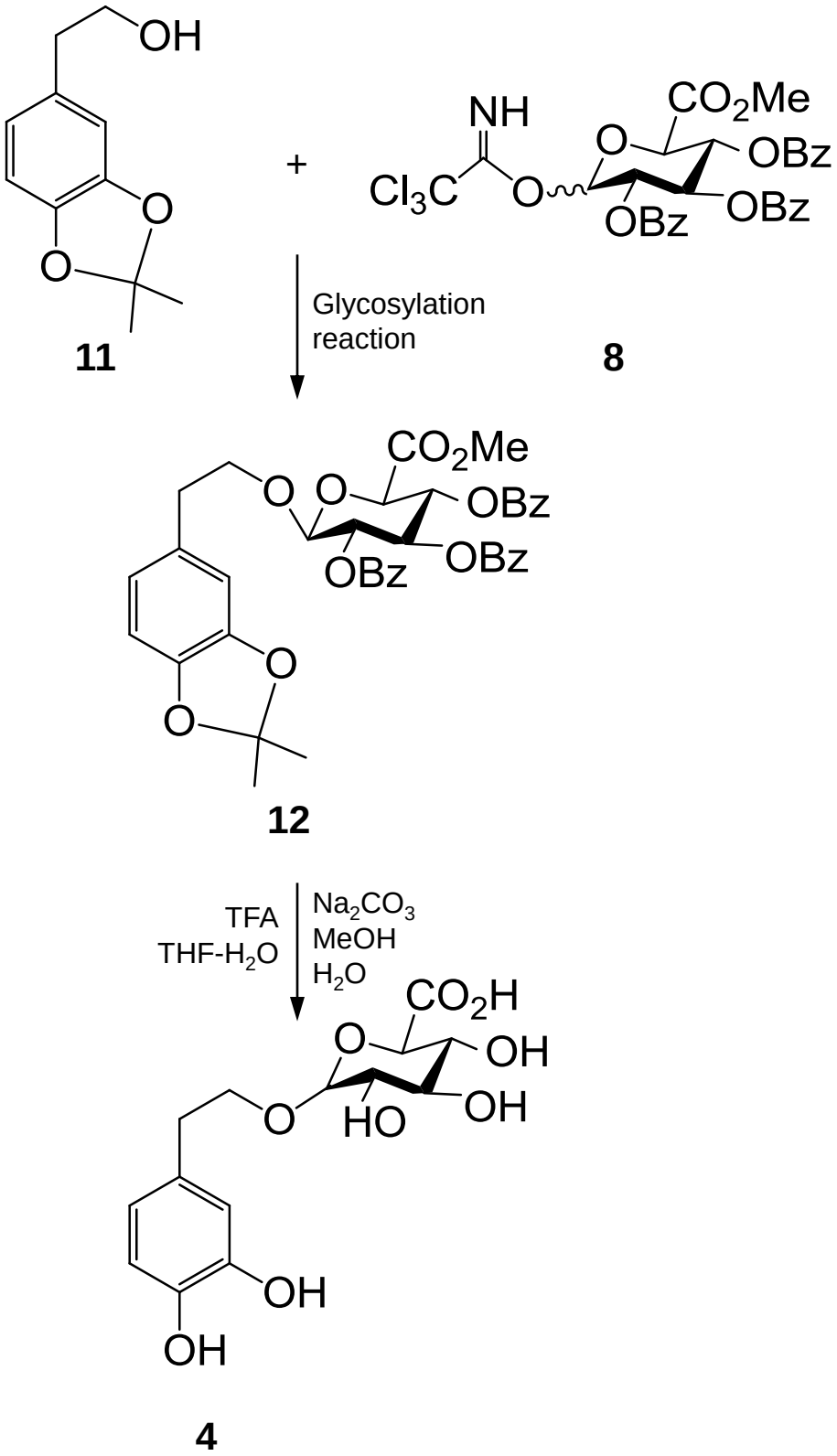
OH
O
O
11
+
NH
Cl3C
O
CO2Me
O
OBz
OBz
OBz
8
Glycosylation
reaction
CO2Me
O
O
OBz
OBz
OBz
O
O
12
TFA
THF-H2O
Na2CO3
MeOH
H2O
CO2H
O
OH
O
HO
OH
OH
OH
4

Scheme 3

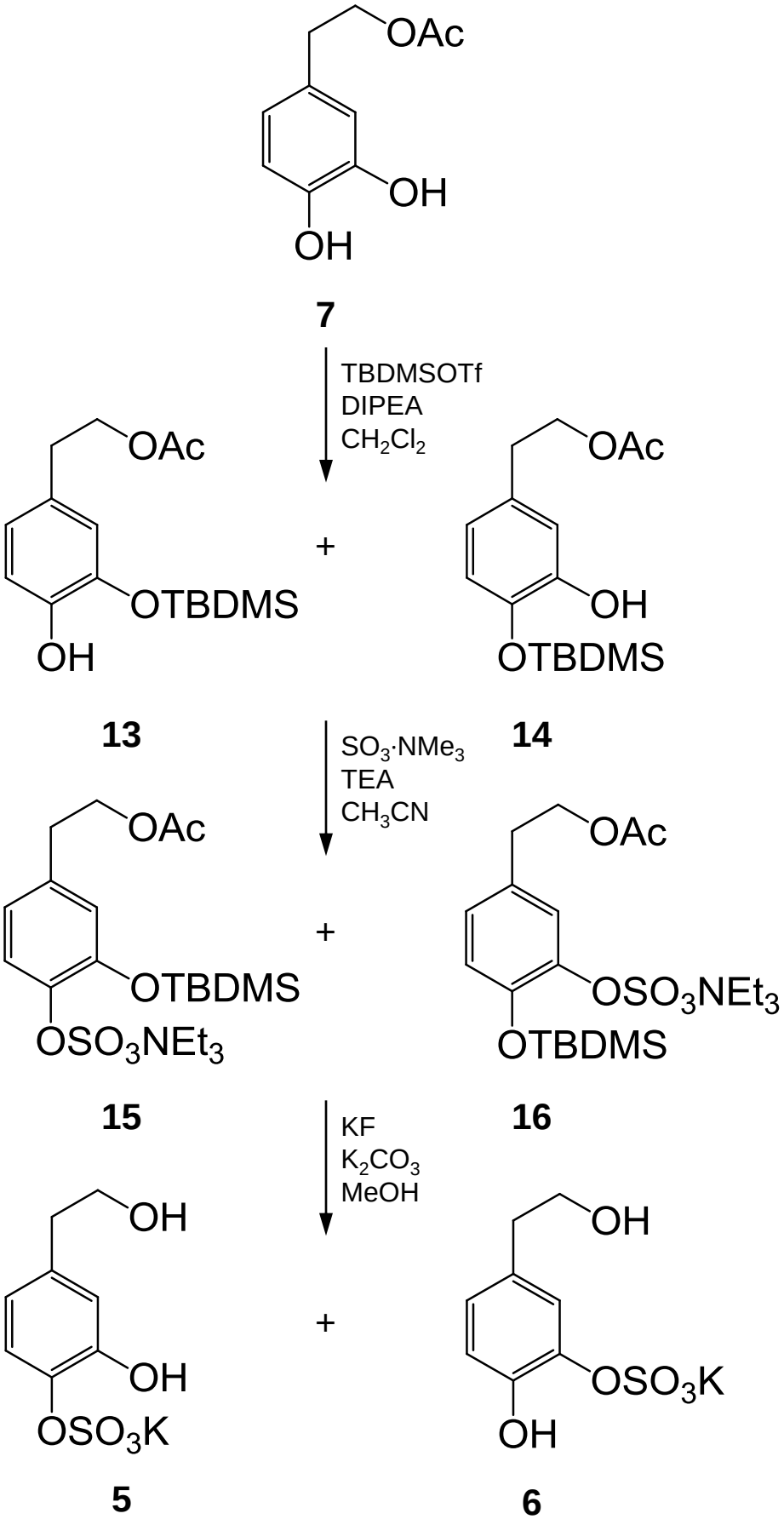
OAc
OH
OH
7
TBDMSOTf
DIPEA
CH_2Cl_2
OAc
OTBDMS
OH
13
+
OAc
OH
OTBDMS
14
$SO_3{\cdot}NMe_3$
TEA
CH_3CN
OAc
OTBDMS
OSO_3NEt_3
15
+
OAc
OSO_3NEt_3
OTBDMS
16
KF
K_2CO_3
MeOH
OH
OH
OSO_3K
5
+
OH
OSO_3K
OH
6

Supplementary material

Effect of metabolites of hydroxytyrosol on protection against oxidative stress and inflammation in human endothelial cells

Sergio Lopez[a,*], Sergio Montserrat-de la Paz[a], Ricardo Lucas[b,c], Beatriz Bermudez[a,d], Rocio Abia[a], Juan C. Morales[b,c], Francisco J.G. Muriana[a,*]

[a]Laboratory of Cellular and Molecular Nutrition, Instituto de la Grasa (CSIC). 41013 Seville, Spain.

[b]Department of Bioorganic Chemistry, Instituto de Investigaciones Químicas (CSIC-Universidad de Sevilla). 41092 Seville, Spain.

[c]Department of Biochemistry and Molecular Pharmacology, Instituto de Parasitología y Biomedicina (CSIC). 18016, Armilla, Granada, Spain.

[d]Department of Cell Biology, School of Biology (University of Seville). 41012 Seville, Spain.

* *Corresponding authors*: Laboratory of Cellular and Molecular Nutrition, Instituto de la Grasa (CSIC), 41013 Seville, Spain. Tel.: +34 954611550; fax: +34 954616790.

E-mail addresses: serglom@ig.csic.es (S. Lopez) delapaz@us.es (S. Montserrat-de la Paz), ricardo.lucas@ipb.csic.es (R. Lucas), bbermudez@us.es (B. Bermudez), abia@ig.csic.es (R. Abia), jcmorales@ipb.csic.es (J.C. Morales), and muriana@ig.csic.es (F.J.G. Muriana).

Materials and methods

1. Synthesis of HTyr glucuronate metabolites

To a solution of HTyr acetate **7** (Grasso, Siracusa, Spatafora, Renis, & Tringali, 2007; Lucas et al., 2010) (200 mg, 1.02 mmol) in anhydrous CH_2Cl_2 (6 mL) and trichloroacetimidate acetylate glucuronosyl donor **8** (Fischer et al., 1984) (366 mg, 0.76 mmol) at −10 °C, $BF_3{\cdot}OEt_2$ (25 μL, 0.19 mmol) was added drop wise. After 2 h, TLC (hexane-EtOAc 2:1) showed the formation of a new product and complete consumption of the glycosyl donor. The reaction was neutralized with NEt_3 and concentrated in vacuum. The resulting residue was purified by flash column chromatography (hexane-EtOAc from 3:1 to 1:1) to afford a regioisomeric mixture of **9** and **10** (205 mg, 51%); ^{1}H NMR (400 MHz, $CDCl_3$) δ 6.89-6.80 (m, 3H, H_{arom}), 6.63 (m, 1H, H_{arom}), 6.19 (m, 2H, H_{arom}), 5.37-5.25 (m, 6H, H-2a, H-2b, H-3a. H-3b, H-4a, H-4b), 5.03, 5.02 (2d, *J* = 7.6 Hz, 2H, H-1a, H-1b), 4.23-4.17 (m, 6H, H-5a, H-5b, 2 × CH_2), 3.74 (s, 6H, CH_3O), 2.84-2.80 (m, 4H, 2 × CH_2), 2.09-2.06 (m, 24H, $CH_3C{=}O$); ^{13}C NMR (100.5 MHz, $CDCl_3$) δ 171.1, 171.0 ($COOCH_3$), 170.0, 169.8, 169.7 169.4, 166.8, 143.9, 142.8, 135.4, 130.0, 125.7, 120.6, 118.3, 118.0, 117.0, 116.5, 101.4, 100.1 (C-1a, C-1b), 72.4, 71.5, 71.4, 71.2, 71.1, 69.0, 68.9, 64.8, 64.7, 53.1, 34.5, 34.2, 20.9, 20.6, 20.5, 20.4. ESIMS: Calcd for $C_{23}H_{28}NaO_{13}Na$: 536.1. Found: 536.8. A solution of the regioisomeric mixture of **9** and **10** (60 mg, 0.11 mmol) in MeOH (2 mL) was stirred at room temperature with a solution of Na_2CO_3 (22 mg, 0.204 mmol) in H_2O (0.5 mL). After 16 h, water (1 mL) was added, followed by addition of glacial acetic acid to adjust the pH to 6.2. The solvents were then removed and residue was purified by Sephadex G-25 eluting with H_2O-MeOH (9:1). Fractions containing the desired product mixture were freeze-dried affording compounds **2** and **3** (32 mg, 88%) as a 1.7:1 regioisomeric mixture; ^{1}H NMR (500 MHz, D_2O) δ 7.00-6.70 (m, 6H,

H_{arom}), 4.97, 4.94 (2d, *J* = 7.0 Hz, 2H, H-1, H-1′), 3.77-3.75 (m, 2H, H-3, H-3′), 3.76-3.52 (m, 10H, H-4, H-4′, H-5, H-5′, CH_2, H-2, H-2′), 2.68-2.64 (m, 4H, CH_2); ^{13}C NMR (75 MHz, D_2O) δ 181.1 175.0 (C=O), 143.8, 143.0, 135.1, 131.9, 124.3, 121.3, 117.4, 117.0, 116.9, 116.4 (C_{arom}), 101.3, 101.0 (C-1, C-1′), 76.3, 75.2, 72.6, 71.7, 62.5, 62.4, 46.5, 37.0. ESIMS: Calcd for $C_{14}H_{15}O_9$ (M^{3-}): 327.1. Found: 327.0.

To a solution of HTyr derivative **11** (Gambacorta, Tofani, Bernini & Migliorini, 2007) (90 mg, 0.46 mmol) in anhydrous CH_2Cl_2 (4 mL) and trichloroacetimidate benzoylate glucuronosyl donor **8** (680 mg, 1.02 mmol) at −10 °C, $BF_3{\cdot}OEt_2$ (66 μL, 0.51 mmol) was added drop wise. After 1 h, the reaction was neutralized with NEt_3 and concentrated in vacuum. The resulting residue was purified by flash column chromatography (toluene-EtOAc from 20:1 to 6:1) to afford **12** (270 mg, 84%); $[\alpha]_D^{22}$ +25.2 (c 1 in $CHCl_3$); ^{1}H NMR (300 MHz, $CDCl_3$) δ 7.89-7.28 (m, 15H, H_{arom}), 6.57-6.40 (m, 3H, H_{arom}), 5.92 (t, *J* = 9.3 Hz, 1H, H-3), 5.72 (t, *J* = 9.6 Hz, 1H, H-4), 5.09 (dd, *J* = 7.5 and 9.3 Hz, 1H, H-2), 4.90 (d, *J* = 7.5 Hz, 1H, H-1), 4.36 (d, *J* = 9.6 Hz, 1H, H-5), 4.15 (m, 1H, OCH_2), 3.74-3.71 (m, 4H, OCH_2, CH_3O), 2.82-2.77 (m, 2H, $PhCH_2$), 1.64, 1.63 (2s, 6H, $C(CH_3)_2$). ^{13}C NMR (75 MHz, $CDCl_3$) δ 167.4, 165.6, 165.2, 165.0 (C=O), 147.3, 145.8 (Cq_{arom}), 133.4, 133.3, 133.2, 131.2, 129.8, 129.0, 128.9, 128.8, 128.7, 128.4, 128.3, 128.2, 125.3, 121.2, 117.5, 109.1, 107.9, 101.0 (C-1), 72.9, 72.1, 71.1, 70.2, 52.9, 35.6, 25.8. ESIMS: Calcd for $C_{39}H_{36}O_{12}Na$: 719.2104. Found: 719.2097. A solution of compound **12** (120 mg, 0.17 mmol) in MeOH (6 mL) was stirred at room temperature with a solution of Na_2CO_3 (110 mg, 1.02 mmol) in H_2O (2.0 mL). After 4 days, water (1 mL) was added, followed by addition of glacial acetic acid to adjust the pH to 6.2. The solvents were then removed and residue was used for the next step without further purification. The latter crude was dissolved in THF-H_2O (1:1, 2 mL) and TFA (3 mL) was then added.

The reaction mixture was stirred at room temperature for 48 h. Solvents were then removed in vacuum and the residue was purified by Sephadex G-25 eluting with H_2O-MeOH (9:1) and RP-C18 eluting with H_2O-CH_3CN (from 100:0 to 70:30). Fractions containing the desired product were freeze-dried affording compound **4** (42 mg, 75%). ^{1}H NMR (300 MHz, D_2O) δ 6.59-6.44 (m, 3H, H_{arom}), 4.19 (d, J = 7.8 Hz, 1H, H-1), 3.79-3.74 (m, 1H, CH_2), 3.62-3.52 (m, 2H, CH_2, H-5), 3.31-3.20 (m, 2H, H-3, H-4), 3.05-2.99 (m, 1H, H-2), 2.56-2.51 (m, 2H, CH_2); δ (75 MHz, D_2O); 163.2, 162.7, 143.8, 142.2, 131.3, 121.1, 116.6, 116.1, 102.1 (C-1), 75.2, 72.7, 71.3, 71.1, 34.3. ESIMS Calcd for $C_{14}H_{15}O_9$ (M^{3-}): 327.0733. Found: 327.0408.

2. Synthesis of HTyr sulfate metabolites

To a solution of HTyr acetate **7** (Grasso, Siracusa, Spatafora, Renis, & Tringali, 2007; Lucas et al., 2010) (223 mg, 1.13 mmol) in DMF (anhydrous, 3 mL) cooled in an ice-water bath under argon were added sequentially tert-butyldimethylsilyl-trifluoromethanesulfonate (TBDMSOTf, 287 μL, 1.25 mmol, 1.10 equiv.) and diisopropylethylamine (DIEA, 265 μL, 1.52 mmol, 1.35 equiv.). The mixture was allowed to stir for 30 min at 0 °C. The completion of the reaction was monitored by TLC (hexane:ethyl acetate; 3:1). The pale yellow reaction mixture was diluted with EtOAc (100 mL), cast into a separatory funnel, and washed with water (2 × 50 mL) and brine (50 mL), and the organic phase was dried (Na_2SO_4). Filtration and concentration in a vacuum afforded the crude extract that was purified by flash column chromatography (hexane:ethyl acetate from 15:1 to 10:1) to afford **13** and **14** (314 mg, 90%, powder) like a regioisomeric mixture in the ratio of ≈1:1. ^{1}H NMR (400 MHz, $CDCl_3$) δ 6.88 (d, 1H, J = 8.1 Hz, H_{arom}), 6.83 (s, 1H, H_{arom}), 6.77 (d, 1H, J = 8.4 Hz, H_{arom}), 6.73 (d, 1H, J = 8.4 Hz, H_{arom}), 6.71 (s, 1H, H_{arom}), 6.62 (d, 1H, J = 8.1 Hz,

H_{arom}), 5.52, 5.45 (2s, 2H, 2 × OH), 4.26 (t, 2H, *J* = 6.7 Hz, CH_2OAc), 4.24 (t, 2H, *J* = 6.4 Hz, CH_2OAc), 2.86 (t, 2H, *J* = 6.7 Hz, CH_2Ar), 2.84 (t, 2H, *J* = 6.4 Hz, CH_2Ar), 2.07-2.05 (2s, 6H, $CH_3C{=}O$), 1.05, 1.03 (2s, 18H, $C(CH_3)_3$ × 2), 0.30, 0.29 (2s, 12H, -$Si(CH_3)_2$ × 2); ^{13}C-NMR (125 MHz, $CDCl_3$) δ: 171.1, 171.0 (C=O), 147.1, 145.9, 142.3, 141.0, 131.8, 129.6 (Cq_{arom}), 122.4, 120.2, 118.6, 117.7, 115.4, 114.8 (CH_{arom}), 65.2, 65.0 (CH_2OAc), 34.5 (2 × CH_2Ar), 25.7 ($C(CH_3)_3$), 21.0, 20.9 ($CH_3C{=}O$), 18.2 ($C(CH_3)_3$), -4.2 (Si-$(CH_3)_2$). HRMS (ES^+) Calcd for $C_{16}H_{26}O_4NaSi$ (M + Na) 333.1498. Found: 333.1508. A regioisomeric mixture of compounds **13** and **14** (157 mg, 0.506 mmol) and $SO_3{\cdot}NMe_3$ (351 mg, 2.52 mmol) were subjected to sulfation conditions for 2 × 20 min. TLC (ethyl acetate:MeOH; 10:1) showed the formation of a major product and complete consumption of the starting material. Solvents were removed and the crude was purified by using Sephadex LH-20 in a solvent mixture of CH_2Cl_2:MeOH (1:1) to afford **15** and **16** (231 mg, 94%, powder) like a regioisomeric mixture in the ratio ≈1:1. ^{1}H-NMR (400 MHz, $CDCl_3$) δ: 7.50 (d, 1H, *J* = 7.9 Hz, H_{arom}), 7.46 (s, 1H, H_{arom}), 6.82 (d, 1H, *J* = 8.2 Hz, H_{arom}), 6.78 (d, 1H, *J* = 8.2 Hz, H_{arom}), 6.73 (d, 1H, *J* = 7.9 Hz, H_{arom}), 6.72 (s, 1H, H_{arom}), 4.20 (t, 4H, *J* = 7.08 Hz, CH_2OAc), 3.10-3.00 (dq, 12H, CH_2CH_3), 2.83 (t, 2H, *J* = 7.1 Hz, CH_2Ar), 2.82 (t, 2H, *J* = 7.05 Hz, CH_2Ar), 2.04, 2.03 (2s, 6H, $CH_3C{=}O$), 1.26 (t, 18H, CH_2CH_3), 1.00, 0.99 (2s, 18H, $C(CH_3)_3$ × 2), 0.21, 0.20 (2s, 12H, -$Si(CH_3)_2$ × 2); ^{13}C-NMR (125 MHz, $CDCl_3$) δ: 171.0, 170.9 (C=O), 146.8, 145.6, 143.9, 142.8, 134.0, 130.7 (Cq_{arom}), 124.5, 122.4, 121.9, 121.8, 121.6, 121.0 (CH_{arom}), 65.1 (CH_2OAc), 46.3 (CH_2CH_3), 34.5 (CH_2Ar), 25.7 ($C(CH_3)_3$), 21.0 ($CH_3C{=}O$), 18.8 ($C(CH_3)_3$), 8.8 (CH_2CH_3), -4.2 ($Si(CH_3)_2$). ESI-HRMS (ES^-) Calcd for $C_{16}H_{25}O_7SiS$ (M - H) 389.1090. Found: 389.1092. A regioisomeric mixture of **15** and **16** (231 mg, 0.47 mmol), potassium fluoride (KF, 55 mg, 0.94 mmol), and potassium carbonate (K_2CO_3, 130

mg, 0.94 mmol) were dissolved in MeOH (10 mL). The reaction mixture was stirred at room temperature for 18 h and the solvent was then removed in a vacuum. The crude extract was purified by column chromatography with RP-C18 silica gel eluting with H_2O:MeOH (from 100:0 to 70:30). Fractions containing the desired product were concentrated and freeze-dried affording compounds **5** and **6** (115 mg, 90%, white powder) like a regioisomeric mixture in the ratio ≈1:1. ^{1}H-NMR (300 MHz, D_2O) δ: 7.21 (d, 2H, *J* = 8.0 Hz, H_{arom}), 7.17 (s, 1H, H_{arom}), 6.98 (d, 1H, *J* = 8.5 Hz, H_{arom}), 6.88 (d, 1H, *J* = 8.5 Hz, H_{arom}), 6.80 (s, 1H, H_{arom}), 6.70 (d, 1H, *J* = 8.0 Hz, H_{arom}), 3.76-3.69 (m, 4H, CH_2OAc), 2.73-2.70 (m, 4H, CH_2Ar); ^{13}C-NMR (125 MHz, D_2O) δ: 149.4, 147.4, 139.0, 138.4, 137.8, 130.7, 127.6, 123.0, 122.6, 120.0, 118.2, 117.6, 62.6, 62.4 (CH_2OAc), 37.4, 36.9 (CH_2Ar). HRMS-ESI (ES^-) Calcd for $C_8H_9O_6S$ (M - H) 233.0120. Found: 233.0126.

Supplementary references

Fischer, B., Nudelman, A., Ruse, M., Herzig, J., Gottlieb, H.E., & Keinan, E. (1984). A novel method for stereoselective glucuronidation. *Journal of Organic Chemistry, 49*(25), 4988-4993.

Gambacorta, A., Tofani, D., Bernini, R., & Migliorini, A. (2007). High-yielding preparation of a stable precursor of hydroxytyrosol by total synthesis and from the natural glycoside oleuropein. *Journal of Agricultural and Food Chemistry, 55*(9), 3386-3391.

Grasso, S., Siracusa, L., Spatafora, C., Renis, M., & Tringali, C. (2007). Hydroxytyrosol lipophilic analogues: enzymatic synthesis, radical scavenging activity and DNA oxidative damage protection. *Bioorganic Chemistry*, *35*(2), 137-152.

Lucas, R., Comelles, F., Alcantara, D., Maldonado, O. S., Curcuroze, M., Parra, J.L., & Morales, J.C. (2010). Surface-active properties of lipophilic antioxidants tyrosol and hydroxytyrosol fatty acid esters: a potential explanation for the nonlinear hypothesis of the antioxidant activity in oil-in-water emulsions. *Journal of Agricultural and Food Chemistry*, *58*(13), 8021-8026.

Table S1. Sequences of primers for gene expression analysis.

Target	GenBank accession number	Direction	Sequence (5'→3')
GPX1	NM_000581	Forward Reverse	AGAATGTGGCGTCCCTCTGA ACCGTTCACCTCGCACTTCT
GCLC	NM_001498	Forward Reverse	TCCAGGTGACATTCCAAGCC GAAATCACTCCCCAGCGACA
HO-1	NM_002133	Forward Reverse	TCTTGGCTGGCTTCCTTACC GGATGTGCTTTTCGTTGGGG
ICAM-1	NM_000201	Forward Reverse	CAGTCACCTATGGCAACGAC ATTCAGCGTCACCTTGGCTC
VCAM-1	NM_001078	Forward Reverse	TCCGTCTCATTGACTTGCAG CACCTGCATTCCTTTTTCCA
E-selectin	NM_000450	Forward Reverse	AGCCCAGAGCCTTCAGTGTA AACTGGGATTTGCTGTGTCC
CCL2	NM_002982	Forward Reverse	CCCCAGTCACCTGCTGTTAT TGGAATCCTGAACCCACTTC
PTGS2	NM_000963	Forward Reverse	TGAGCATCTACGGTTTGCTG TGCTTGTCTGGAACAACTGC
GAPDH	NM_001289746	Forward Reverse	TCGACAATGGCAGCATCTAC ATCCGTCTCCACAGACAAGG
HPRT	NM_000194	Forward Reverse	ACCCCACGAAGTGTTGGATA AAGCAGATGGCCACAGAACT

Table S2. Concentration of soluble forms of ICAM-1, VCAM-1, and E-selectin in the medium of hECs.

Treatment	sICAM-1	sVCAM-1	sE-selectin
Control	2.0 ± 0.6^{a}	1.2 ± 0.7^{a}	3.7 ± 0.5^{b}
TNF-α	6.4 ± 1.0^{b}	9.6 ± 1.0^{b}	6.7 ± 1.0^{c}
HTyr + TNF-α	2.4 ± 0.8^{a}	1.0 ± 1.8^{a}	1.4 ± 0.8^{a}
HTyr-GLU + TNF-α	3.1 ± 1.5^{a}	1.8 ± 1.5^{a}	3.6 ± 1.5^{b}
HTyr-*O*-GLU + TNF-α	2.9 ± 0.9^{a}	2.6 ± 1.0^{a}	3.3 ± 1.1^{b}
HTyr-SUL + TNF-α	2.4 ± 0.7^{a}	2.1 ± 1.4^{a}	3.1 ± 0.8^{b}

hECs were untreated (control) or exposed to hydroxytyrosol (HTyr), hydroxytyrosol glucuronate metabolites (HTyr-GLU and HTyr-*O*-GLU), and hydroxytyrosol sulfate metabolites (HTyr-SUL) (all 100 μM for 16 h) and then with TNF-α (10 ng/mL) for additional 16 h. Values are expressed in pg/mL and are shown as the mean ± SD (n = 3). Values within columns without a common superscript lowercase letter differ ($p < 0.05$).

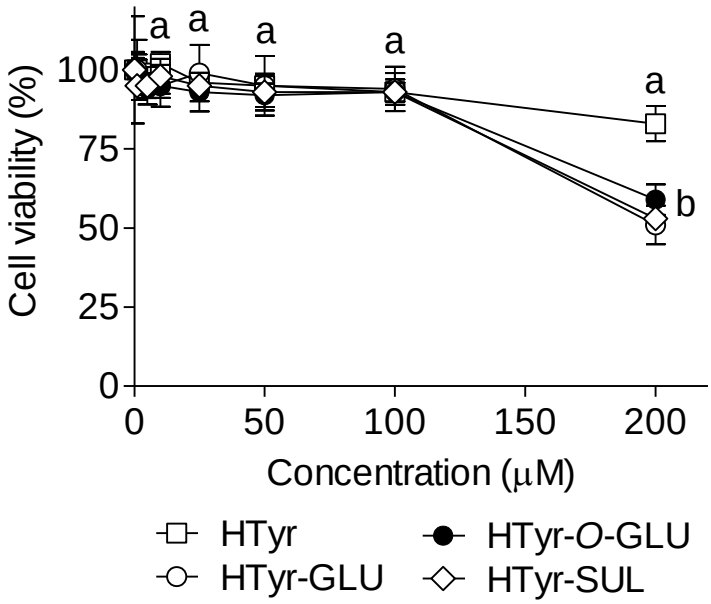

Figure S1. Effects of hydroxytyrosol (HTyr), hydroxytyrosol glucuronate metabolites (HTyr-GLU and HTyr-*O*-GLU), and hydroxytyrosol sulfate metabolites (HTyr-SUL) on hEC viability. Cells were cultured in the presence of HTyr and HTyr metabolites (0-200 μM) for 48 h. Values are shown as the mean ± SD (n = 8). Means without a common lowercase letter differ ($p < 0.05$).

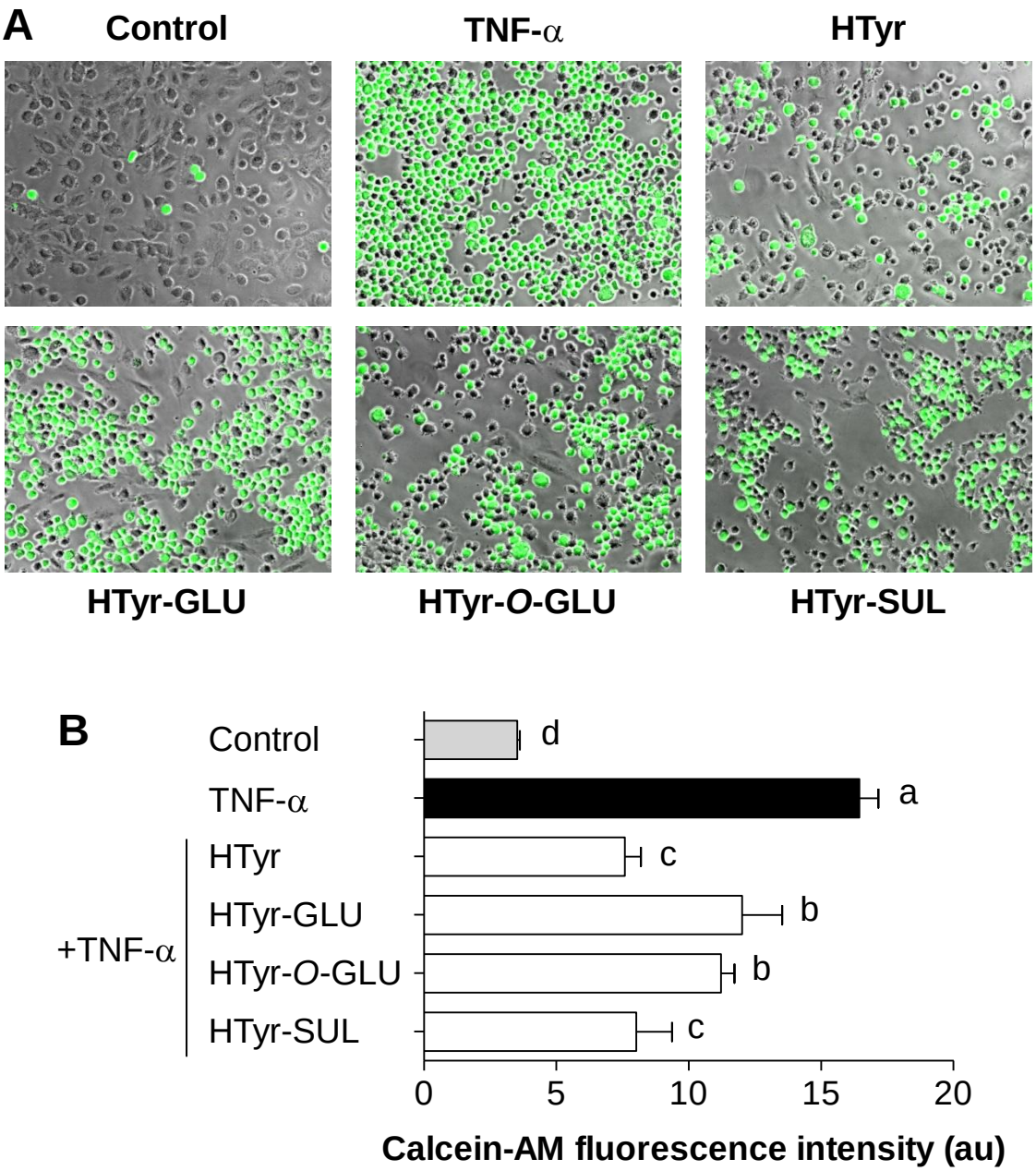

Figure S2. Effects of hydroxytyrosol (HTyr), hydroxytyrosol glucuronate metabolites (HTyr-GLU and HTyr-*O*-GLU), and hydroxytyrosol sulfate metabolites (HTyr-SUL) (all 100 μM for 16 h) on adherence of calcein-AM-labeled THP-1 monocytes (A, representative photomicrographs; B quantitative analysis) to TNF-α-treated hECs. Values are shown as the mean ± SD (n = 3). Bars without a common lowercase letter differ ($p < 0.05$).